ARISTOTLE UNIVERSITY OF THESSALONIKI
Interinstitutional Program of Postgraduate Studies in
PALAEONTOLOGY – GEOBIOLOGY

Christos Tsakalidis
Geologist

MESOWEAR DIETARY COMPARISON AMONG GREEK ELEPHANTIDAE (MAMMUTHUS AND PALAEOLOXODON)

MASTER THESIS

DIRECTION: Macropalaeontology
Directed by: Aristotle University of Thessaloniki

THESSALONIKI
2024

[λευκή σελίδα]

Interinstitutional
Program of
Postgraduate
Studies in
PALAEONTOLOGY – GEOBIOLOGY

supported by:

SCHOOL OF GEOLOGY AUTH

Τμήμα Γεωλογίας ΑΠΘ
School of Geology AUTh

school of biology

Τμήμα Βιολογίας ΑΠΘ
School of Biology AUTh

National and Kapodistrian

University of Athens

Faculty of Geology and Geoenvironment

Τμήμα Γεωλογίας & Γεωπεριβάλλοντος
ΕΚΠΑ
Faculty of Geology & Geoenvironment
NKUA

Department of GEOLOGY

Τμήμα Γεωλογίας Παν/μίου Πατρών
Department of Geology, Patras Univ.

UNIVERSITY OF THE AEGEAN

Τμήμα Γεωγραφίας Παν/μίου Αιγαίου
Department of Geography, Aegean Univ.

[λευκή σελίδα]

Christos Tsakalidis
Χρήστος Τσακαλίδης
Πτυχιούχος 2024

MESOWEAR DIETARY COMPARISON AMONG GREEK ELEPHANTIDAE (MAMMUTHUS AND PALAEOLOXODON)

ΔΙΑΤΡΟΦΙΚΕΣ ΣΥΓΚΡΙΣΕΙΣ ΜΕΤΑΞΥ ΜΕΛΩΝ ΤΗΣ ΟΙΚΟΓΕΝΕΙΑΣ ΤΩΝ ELEPHANTIDAE (MAMMUTHUS ΚΑΙ PALAEOLOXODON) ΜΕΣΩ ΜΕΣΟΤΡΙΒΗΣ

Υποβλήθηκε στο ΔΠΜΣ Παλαιοντολογία-Γεωβιολογία

Ημερομηνία Προφορικής Εξέτασης: 01/03/2024
Oral Examination Date: 01/03/2024

Three-member Examining Board

Dr. George E. Konidaris, Supervisor
Professor Dimitrios S. Kostopoulos, Member
Em. Professor Evangelia Tsoukala, Member

Τριμελής Εξεταστική Επιτροπή

Δρ. Γεώργιος Κονιδάρης, Επιβλέπων
Καθηγητής Δημήτριος Σ. Κωστόπουλος, Μέλος Τριμελούς Εξεταστικής Επιτροπής
Ομ. Καθηγήτρια Ευαγγελία Τσουκαλά, Μέλος Τριμελούς Εξεταστικής Επιτροπής

External Assistant/Εξωτερικός Συνεργάτης (σύμφωνα με ΕΔΕ5/15-7-2019)
Dr. Athanasios Athanassiou

MESOWEAR DIETARY COMPARISON AMONG GREEK ELEPHANTIDAE (MAMMUTHUS AND PALAEOLOXODON)
Master Thesis

ΔΙΑΤΡΟΦΙΚΕΣ ΣΥΓΚΡΙΣΕΙΣ ΜΕΤΑΞΥ ΜΕΛΩΝ ΤΗΣ ΟΙΚΟΓΕΝΕΙΑΣ ΤΩΝ ELEPHANTIDAE (MAMMUTHUS ΚΑΙ PALAEOLOXODON) ΜΕΣΩ ΜΕΣΟΤΡΙΒΗΣ
Μεταπτυχιακή Διπλωματική Εργασία

Citation:
Tsakalidis C., 2024 – PALAEODIETARY INFERENCES BASED ON DENTAL MESOWEAR ANALYSIS OF PLIO-PLEISTOCENE PROBOSCIDEANS FROM GREECE. Master Thesis, Interinstitutional Program of Postgraduate Studies in Palaeontology-Geobiology. School of Geology, Aristotle University of Thessaloniki, 79 pp.

Cover Figure: Larramendi et al. (2017)

Acknowledgements

I would like to express my deepest gratitude to my supervisor, Dr. George Konidaris for his invaluable help, guidance, and unwavering support throughout the entirety of this research journey. His expertise, insightful feedback, organizing skills and patience have been instrumental in shaping this thesis.

I also want to thank the members of the examining board Prof. Dimitris Kostopoulos for his comments and suggestions that enriched the final text as well as for organizing the visit to the Historical Palaeontological Collection of Siatista, and the Palaeontological and Historical Museum of Ptolemaida, and Professor Evangelia Tsoukala for her comments on the manuscript, as well as for granting me access to the Historical Palaeontological Collection of Siatista. Special acknowledgement is owed to the external assistant Dr. Athanasios Athanassiou for his constructive criticism and his attention to details that improved both my scientific thinking and writing skills.

Furthermore, I extend my sincere appreciation to the faculty and staff of the Ephorate of Antiquities of Achaia (Patras) for granting me access to the Loussika specimen, especially Konstantina Aktypi, as well as Dr. Athanasios Athanassiou for organizing this visit. Moreover, I would like to thank Prof. Eyterpi Koskeridou (Faculty of Geology and Geoenvironment, NKUA) for granting me access to the specimens stored in the Museum of Palaeontology and Geology at Athens and Assoc. Prof. Sokratis Roussiakis (NKUA) for all the help in the collection and for his willingness to provide assistance throughout my stay at the museum.

Excavation at Marathousa 1 (Megalopolis Basin) was conducted under a permit granted to the Ephorate of Palaeoanthropology–Speleology, Hellenic Ministry of Culture and was supported by the ERCStG-283503 ("PaGE") and the ERC-CoG-724703 (“CROSSROADS”), both awarded to K. Harvati. The 2018–2021 field survey in the Megalopolis Basin (including the inspection of the site Kyparissia-3) was conducted in the framework of the Megalopolis Palaeoenvironmental Project (MegaPal) under a permit granted to the Ephorate of Paleoanthropology–Speleology, Hellenic Ministry of Culture, and the American School of Classical Studies at Athens; it was supported by the ERC Consolidator Grant ERC-CoG-724703 (“CROSSROADS”), awarded to K. Harvati.

Last but not least, I am immensely thankful to my family, friends and colleagues for their encouragement, discussions, and moral support throughout this process, as well as to everyone that helped with the transportation of these massive specimens, I was lucky to examine.

Abstract

Analyzing the dental wear of extinct herbivorous mammals, particularly megaherbivores, provides important palaeodietary insights that significantly contribute to the reconstruction of palaeoenvironments. In this thesis the dental mesowear angle method is employed on elephants and mammoths from Pliocene and Pleistocene localities of Greece, in order to classify them into three main dietary categories (browsers, mixed feeders, and grazers), and provide data regarding their dietary preferences as well as indicate cases of potential niche partitioning. The method relies on documenting the wear pattern of molar surfaces through angle measurements on the enamel ridges which reflect the average annual diet of the examined taxon and in turn the annual ecological conditions of the studied area. In order to ensure the validity of the dental mesowear results, a taxonomic review of the examined specimens was also conducted.

The studied material belongs to the mammoths *Mammuthus rumanus*, *Mammuthus* cf. *rumanus, Mammuthus meridionalis*, and *Mammuthus trogontherii*, and the elephant *Palaeoloxodon antiquus*, and originates from several localities in northern (Ptolemais Basin, Mygdonia Basin, Philippi–Drama Basin, and Haliakmon river-system) and southern (Megalopolis Basin, Loussika, Roupaki) Greece. Results indicate a grazing diet for *M.* (cf.) *rumanus*, mainly a browsing diet for the southern mammoth and a grazing one for the steppe mammoth, and a wide diet spectrum for the straight-tusked elephant, including browsing, mixed-feeding and grazing, depending on the locality. The results highlight the importance of mesowear analysis on proboscidean teeth for palaeodietary and palaeoenviromental inferences, especially when coupled with other proxies such as dental microwear and stable isotope analyses.

Περίληψη

Οι αναλύσεις της οδοντικής αποτριβής εξαφανισμένων θηλαστικών, ειδικά των μεγαλόσωμων φυτοφάγων ζώων, παρέχουν σημαντικές παλαιοδιατροφικές πληροφορίες, οι οποίες συμβάλλουν σημαντικά στην ανασύσταση των παλαιοπεριβαλλόντων. Στην παρούσα διατριβή εφαρμόζεται η μέθοδος της οδοντικής μεσοτριβής σε ελέφαντες και μαμούθ από πλειοκαινικές και πλειστοκαινικές θέσεις της Ελλάδας ώστε να διαχωριστούν στις τρεις κύριες διατροφικές κατηγορίες των φυτοφάγων (θαλλοφάγοι – “browsers”, ποηφάγοι – “grazers”, και ενδιάμεσου τύπου – “mixed feeders”), να συλλεχθούν δεδομένα που αφορούν τις διατροφικές τους συνήθειες, καθώς και να εντοπισθούν πιθανές περιπτώσεις διαχωρισμού θώκων. Η μέθοδος βασίζεται στην καταγραφή των μορφών; μορφοτύπων; φθοράς στις επιφάνειες των γομφίων μέσω μετρήσεων των γωνιών που σχηματίζουν τα τοιχώματα της αδαμαντίνης, οι οποίες αντιστοιχούν στη μέση ετήσια διατροφή και κατ΄ επέκταση στις ετήσιες οικολογικές συνθήκες της περιοχής μελέτης. Προκειμένου να εξασφαλισθεί η εξαγωγή ασφαλών αποτελεσμάτων από τη μεσοτριβή, πραγματοποιήθηκε επιπλέον ταξινομική ανασκόπηση των υπό μελέτη δειγμάτων.

Το υλικό μελέτης ανήκει στα μαμούθ *Mammuthus rumanus*, *Mammuthus* cf. *rumanus, Mammuthus meridionalis* και *Mammuthus trogontherii*, και τον ελέφαντα *Palaeoloxodon antiquus* και προέρχεται από διάφορες θέσεις της βόρειας (λεκάνη Πτολεμαΐδας, λεκάνη Μυγδονίας, λεκάνη Φιλίππων–Δράμας και το ποτάμιο σύστημα του Αλιάκμονα) και νότιας (λεκάνη Μεγαλόπολης, Λουσικά, Ρουπάκι) Ελλάδας. Τα αποτελέσματα δείχνουν grazing διατροφή στο *M. rumanus*, κυρίως browsing στο *M. meridionalis,* κυρίως grazing στο *M. trogontherii* και διατροφή που καλύπτει όλο το διατροφικό φάσμα στο *P. antiquus* ανάλογα με τη θέση. Τα αποτελέσματα αναδεικνύουν τη σημασία της ανάλυσης της μεσοτριβής δοντιών προβοσκιδωτών στην εξαγωγή παλαιοδιατροφικών και παλαιοπεριβάλλοντικών συμπερασμάτων, ειδικά όταν αυτά συνδυάζονται με άλλες μεθόδους, όπως αναλύσεις οδοντικής μικροτριβής και σταθερών ισοτόπων.

CONTENTS

1. Introduction

1.1. Evolution and distribution of Elephantidae with emphasis on European taxa

1.2. Dental wear in herbivores with emphasis on Elephantidae

1.3. Palaeodiet proxy methods

2. Scope of study

3. Materials and methods – Fossiliferous localities

3.1 Materials and Methods

3.2 Abbreviations

3.3 Fossiliferous localities

4. Systematic palaeontology

5. Dental mesowear analysis – Results

6. Comparisons and discussion

7. Conclusions

8. References

9. Appendix

1. Introduction

Extant elephants, stately and powerful mammals, standing at a height of three meters or more and weighing over six tonnes, comprise the last remaining land giants. Only three species of elephants exist today: the African forest elephant (*Loxodonta cyclotis*) in African forests, the African savannah elephant (*Loxodonta africana*) found in sub-Saharan grasslands and woodlands, and the Asian elephant (*Elephas maximus*) with three subspecies inhabiting mixed habitats in India, Sri Lanka, and parts of Southeast Asia (Palombo et al., 2010). These species are the last surviving members of the order Proboscidea. The evolutionary history of proboscideans started in Africa during the Early Eocene, at ~55.0 Ma, if not even earlier during the Late Paleocene (Gheerbrant et al., 1996), and during the Miocene–Pleistocene multiple migration events outside the African continent led to their dispersal and diversification in all continents except Australia and Antarctica (Fischer, 2009). The order has an extensive fossil record comprising more than 180 species and subspecies, 42 genera, and 10 families (Shoshani and Tassy, 2005). Fossil proboscideans have been discovered in both the Old and New World, occupying various habitats such as grasslands, savannas, steppes, lake shores, swamps, mountains, tundra, forests, and deserts (Palombo et al., 2010).

Both the living and most of the extinct members are characterized by a series of distinct features, including their most notable character, the presence of a long, muscular and mobile trunk (or proboscis, from which the name proboscidean originated) formed by the fusion of the upper lip and nose, allowing for versatile functions such as grasping, manipulation, sensory perception, sound production and breathing (Shoshani, 1998; Lister and Bahn, 2007). Many members (excluding the first and most primitive taxa) of the order possessed elongated, curved upper tusks (enlarged upper second incisors), which serve various purposes including defense and manipulation, and by continuously growing throughout their lives, they provide a temporally structured record of diet, climate, behavior, growth, and life history (Fisher, 2009). Proboscideans are also known for their large size, with massive bodies and limbs adapted for supporting their immense weight (Larramendi, 2015). As herbivores, they primarily consume vegetation, including leaves, grasses, bark, and fruits, and their foraging activities have far-reaching consequences for the structure and diversity of associated communities rendering them "keystone megaherbivores" (Owen-Smith, 1987).

The fossil record of proboscideans showcases a rapid evolution (especially during the Pleistocene) which is generally interpreted as a response to environmental shifts and biotic interaction dynamics (competition and co-evolution) (Palombo et al., 2010). These changes were particularly prominent during key climatic transitions, such as the notable climatic shifts over the last 2.6 million years (Palombo et al., 2010) that affected tremendously the evolution of Elephantidae (Fig. 1), including its members in the European continent.

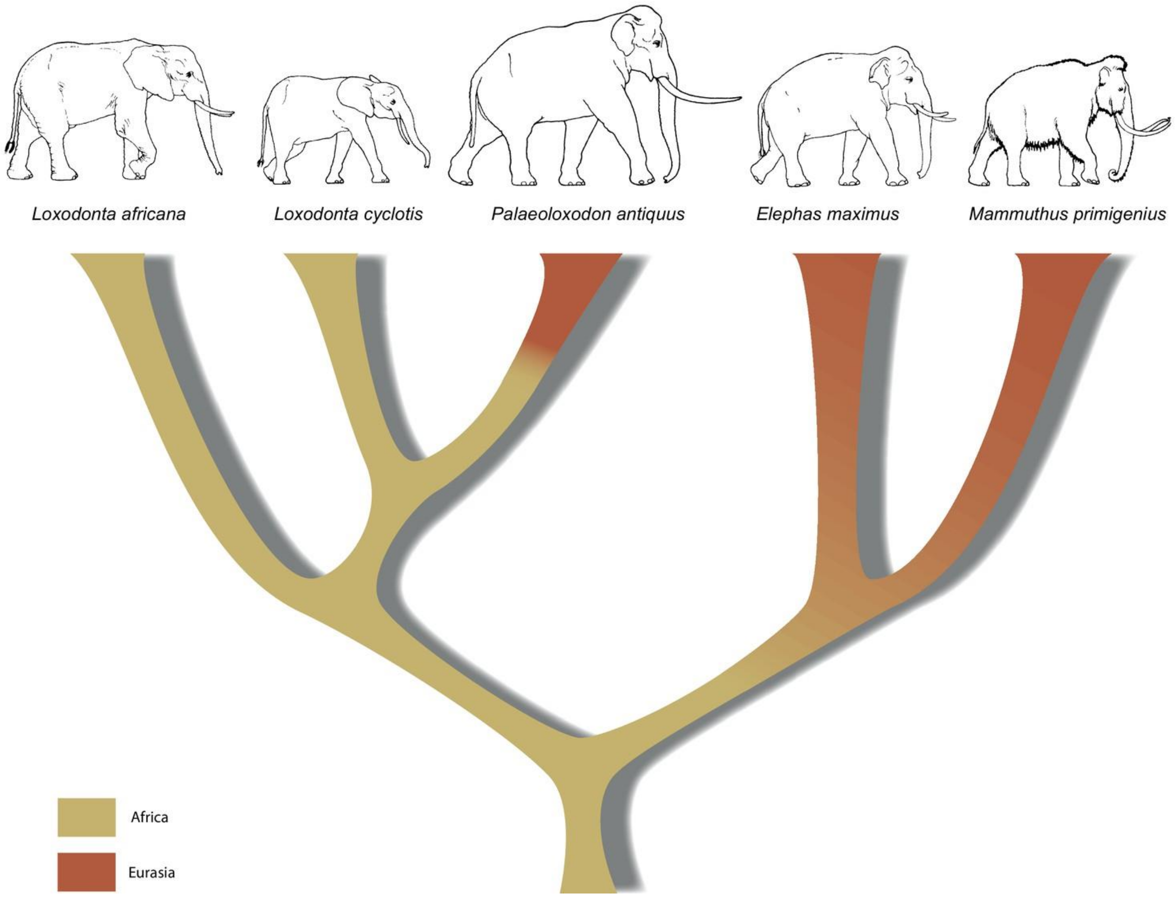

Figure 1. Phylogenetic tree depicting the relationships among specific elephantids, color-coded by their presumed geographical range (taken from Meyer et al., 2017).

1.1 Evolution and distribution of Elephantidae with emphasis on European taxa

The family Elephantidae (genera *Stegotetrabelodon*, *Primelephas*, *Loxodonta*, *Mammuthus*, *Elephas*, and *Palaeoloxodon*) is part of the third main radiation Proboscidea underwent at the end of the Miocene and the Plio-Pleistocene (Shoshani and Tassy, 1996, 2005). The emergence of Elephantidae is generally linked to the major climatic changes towards more open and arid environmental conditions, including the expansion of C_4 plants, namely grasses and sedges (Cerling and Quade, 2013). These environmental changes resulted in the reduction of mammutids and gomphotheriids which in turn "released" ecological niches that were free for elephantids to occupy, if certain anatomical adaptations to a grazing lifestyle were acquired (Sanders, 2010). These modifications include the reconfiguration of craniodental anatomy, transitioning from the grinding-shearing mastication observed in gomphotheres to a specialized fore-aft power-shearing movement of the jaws during feeding, the shortening of the rostral parts of the skull and the mandible, the elevation of parietals and occipitals and the cranium in general, the loss of lower tusks, the shift from lophids to lamellae (plates) in the cheek teeth, the increased lamellar frequency, the higher hypsodonty index, the more complex enamel folding, and the delayed sequential, oblique eruption of cheek teeth (Maglio, 1973; Lister, 1996; Sanders, 2010).

The first representatives of mammoths (*Mammuthus subplanifrons*) appeared at the Miocene/Pliocene boundary in Africa (Sanders et al., 2011). Towards the end of the Pliocene, the Levantine corridor opening gave the opportunity to a plethora of mammals (including elephantids) to migrate from Africa to Eurasia (Palombo, 2010). These migrations were not constricted to a specific time period, but on the contrary, there had been "migration waves" from Africa to Eurasia, with the first wave taking place around 3.5 and 3.0 Ma, including the dispersal of primitive mammoth taxa (Lister et al., 2005; Rabinovich and Lister, 2017).

Mammuthus rumanus is the oldest representative of the genus in Eurasia, which first appears in Europe during the Late Pliocene, between 3.5 and 3.0 Ma (Markov et al., 2012). It is recorded mainly in fossiliferous sites of eastern Europe (Romania, Russia, and Greece), but it is also known from Italy and Great Britain. *Mammuthus rumanus* features primitive characteristics such as brachyodont teeth, low number of lamellae and thick enamel on the molars (Lister et al., 2012). In Greece, the record of *M. rumanus* is rather poor, documented only at Tsotylion, and perhaps at Polylakkos and Kardia, in all cases from imprecise stratigraphic layers (Koulidou, 2013; Kostopoulos and Koulidou, 2015).

The southern mammoth, *Mammuthus meridionalis*, exhibits a distinctive cranium characterized by a dorsally expanded occipital and parietals (Lister et al., 2005). The molars are characterized by more hypsodont crowns with a slightly increased number of plates and lamellar frequency, and thinner enamel compared to *M. rumanus*. The species is quite common and widespread, known from hundreds of localities across Eurasia, except for its northernmost regions. The species is recorded from the middle Villafranchian (Early Pleistocene, ca. 2.6 Ma) and survived until the Epivillafranchian, close to the Early/Middle Pleistocene transition (Lister et al., 2005; Konidaris et al., 2020). In Greece, the species is known from more than 20 Lower Pleistocene localities (Athanassiou, 2022).

The oldest record of the steppe mammoth, *Mammuthus trogontherii*, is documented in China, dating back to the Early Pleistocene, ca. 1.7–1.6 Ma (Wei et al., 2010), and is indicative of an East Asian center for the species' evolution and dispersion (Lister et al., 2005, Lister and Sher, 2015). Subsequent eastern dispersal is evidenced by its presence in the early Olyorian of Siberia, at ca. 1.2–0.8 Ma, and a migration into Europe during the post-Jaramillo–pre-Brunhes interval, potentially involving interbreeding with indigenous populations of *M. meridionalis* (Lister et al., 2005; Van Essen, 2011). The earliest firmly established occurrence of *M. trogontherii* in Europe is traced at Kostolac (Serbia), dated to ca. 0.8 Ma (Lister et al., 2012; Muttoni et al., 2015). Subsequently, *M. trogontherii* is meticulously documented during the early Middle Pleistocene in several localities including West Runton (England; Lister and Stewart, 2010), Süßenborn and Mosbach 2 (Germany; Lister, 2022). In Greece, *M. trogontherii* is rare and mostly limited to the northern regions of the country (Athanassiou, 2022). Yet, a partial skeleton from Loussika (NW Peloponnese) adds to the scarcity of known *M. trogontherii* skeletons in Europe and expands the species' palaeobiogeographic range in the southern Balkans (Athanassiou, 2012).

During the late Olyorian (800–600 ka) north-east Eurasian *M. trogontherii* populations underwent a transformative process leading to more advanced mammoth forms, giving rise to the woolly mammoth *Mammuthus primigenius* (Lister et al., 2005, Kahlke, 2014, Lister & Sher 2015). The emergence of *M. primigenius* in Europe occurred close to the boundary of Marine Isotope Stages (MIS) 7/6, at ca. 200 ka (Lister, 2022). During the Last Cold Stage, the woolly mammoth occupied a vast geographic range, extending across much of Europe, northern Asia, and the northern regions of North America (Stuart et al., 2002). As a species adapted to cold environments, *M. primigenus* is exceptionally rare in Greece, and its presence is linked to glacial periods (Athanassiou, 2022). Similar to other mammoth species, *M.*

primigenus is primarily documented by isolated molars, found in regions of northern Greece, such as the Late Pleistocene localities Angitis and Philippi (Athanassiou, 2022).

Originated in Africa, the straight-tusked elephant, *Palaeoloxodon*, dispersed out of the continent during the Early Pleistocene and through the Levantine corridor reached Europe at the beginning of the Middle Pleistocene (Saegusa and Gilbert, 2008; Palombo et al., 2010; Muttoni et al., 2015). Its initial presence in Europe is recorded with the species *Palaeoloxodon antiquus* at Slivia (Italy), dated close to the Brunhes/Matuyama magnetic polarity boundary, at 0.78 Ma (Palombo, 2014; Muttoni et al., 2018), marking the beginning of the Galerian large mammal age. Throughout the Middle and Late Pleistocene, *P. antiquus* was widely distributed across central and southern Europe (Palombo et al., 2010). *Palaeoloxodon antiquus* stands out as the predominant elephantine species in the Pleistocene of southern Europe, extending its habitat northward during the warmer climatic periods of the Middle Pleistocene. This species is prevalent in numerous locations across Europe, notably abundant in Germany and France, as well as in the refugia of the Italian, Balkan, and Iberian peninsulas during glacial stages (Palombo et al., 2010). The species' wide distribution (Fig. 2), coupled with knowledge of its preferred habitat (mild humid, warm to warm-temperate and wooded environments) and their migration patterns, render *P. antiquus* an important biostratigraphic and palaeoenvironmental proxy (Stuart, 2005; Palombo et al. 2010). Although *P. antiquus* survived numerous glacial periods, the transition from the Last Interglacial to the Last Glacial (MIS 5a) heavily reduced the available habitats and consequently their populations (Palombo et al., 2010). This resulted in its extinction from central and western Europe in the post-Eemian (MIS 5e) period, with some populations surviving until ca. 35 ka (Mol, 2007; Palombo et al., 2010; Athanassiou, 2011).

In Greece, the species is also widespread and documented in more than 20 localities (Tsoukala et al., 2011; Athanassiou, 2022). Notable records are the three partial skeletons of Ambelia, Perdikkas and Marathousa 1 (Tsoukala and Lister, 1998; Tsoukala et al., 2011; Konidaris et al., 2018; Athanassiou, 2022). Yet, besides the Ambelia and Marathousa 1 records, most other findings of *P. antiquus* in Greece lack precise stratigraphic and chronological information, allowing only a general placement within the Middle and Late Pleistocene (Athanassiou, 2022). The last occurrence of the species in Greece, and one of the last in Europe is documented at Pineios river, Thessaly (Athanassiou, 2011).

Figure 2. Localities with presence of *Palaeoloxodon antiquus* (taken from Palombo et al., 2010).

1.2 Dental wear in herbivores with emphasis on Elephantidae

The elephantid molars are comprised of the root and the crown, the latter formed by dentine plates, surrounded by enamel, and joined together with cement (Fig. 3). The plate number depends on the molar position in the dental series, the wear stage, and the taxon. Differentiations in the number of plates, lamellar frequency, enamel thickness and hypsodonty imply dietary differences, as well as differences in the preferred residences (Lister, 2004). The change in the shape of the molars' occlusal surface is caused both by the contact between the teeth of the upper and lower jaw during mastication, and simultaneously by the characteristic wear patterns caused by the plant parts included in the animal's diet, as well as dust particles and gravel (Rivals et al., 2012). The natural properties of the plants consumed by proboscideans tend to wear the molars, and eventually reduce their height, thus reducing their functionality in the long run (Rivals et al., 2012). Both the pattern and the amount of molar wear differ among taxa and even between individuals of the same taxon. These patterns are affected mainly by two different processes, attrition (tooth-to-tooth contact) and abrasion (tooth-to-food contact), which, although independent, occur simultaneously from the grinding that occurs due to the jaw movement during the mastication process (Saarinen and Lister, 2016).

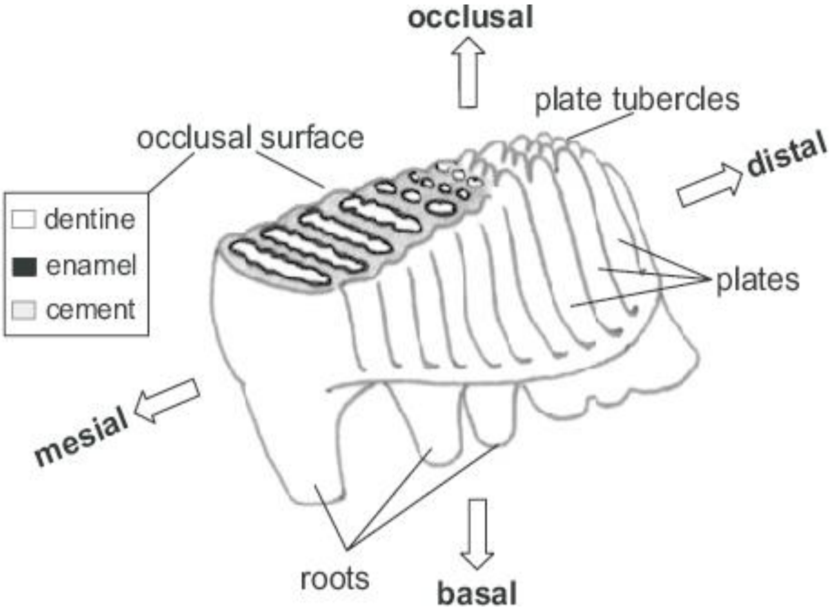

Figure 3. Morphology of Elephantidae molars (taken from Ferretti, 2003).

If the individual prefers to consume soft plant material, the contact between the upper and lower molars increases and thus attrition wear is predominant. On the contrary, abrasion is predominant when the animal's diet includes plants containing abrasive particles of minerals, such as silica or dust particles (in the case of dry environments), which damage the tooth during mastication, causing greater and deeper wear (Kaiser and Solounias, 2003). In pure grazing herbivores, the plant material itself has been found to contribute more to dental wear than the actual tooth to tooth contact and tends to inflict a large number of scratches on the molars. In contrast, attrition creates sharp enamel surfaces that generally appear in browsing organisms (Rivals et al., 2012). Both the degree and the type of wear are important factors to the survival of the individual, as the excessively worn molar plates prevent the acquisition and processing of food, resulting in smaller volume of food intake, and subsequently to minimal nutrient absorption (Lucas et al., 2013). For the body to balance the deficit, the individual is forced to either waste more time in finding and consuming food or to chew more, further wearing its molars, with final consequence the deterioration of its physical condition and the ability to reproduce (Capalbo et al., 2018).

In general, the dental wear grade of herbivore molars (and proboscideans in particular) is heavily influenced by their dietary preferences and, therefore, provides crucial information on both the palaeodiets of extinct species and the palaeoenvironment of certain areas at specific time periods (Rivals et al., 2007). Dental wear patterns reveal the type of food items that was consumed by an individual/taxon, thus, their study methods constitute important tools to determine palaeodiets, particularly because, as taxon-independent methods, they are not affected by the tooth morphology variations of the different species (Rivals et al., 2019). In order to quantify dental wear, palaeontologists utilize primarily micro- and mesowear analyses, which are expanded upon below.

1.3 Palaeodiet proxy methods

As with other megaherbivores, proboscideans have remained very popular for palaeoecological studies because of their role as ecosystem engineers (Haynes, 2012). They are known to be involved in modifying vegetation structure, dispersal of seeds, and recycling and spreading nutrients (Bakker et al., 2016). Consequently, knowledge of their dietary behavior is of importance for gaining insight into the role of these animals in past ecosystems. There are several methods for deciphering the dietary habits of extinct mammals. The most commonly employed are the calculation of the hypsodonty index, as well as the stable isotopes, dental microwear and dental mesowear analyses. These are briefly presented below with emphasis on dental mesowear analysis, which is the focus of this thesis.

Hypsodonty Index: The measurement of crown height in teeth, known as hypsodonty, has been widely used as a dietary indicator, particularly in ruminant artiodactyls (Barr, 2018). The hypsodonty index, calculated in the case of elephantids by dividing the width of an unworn third lower molar plate by its height, helps to understand this dental characteristic (Janis, 1988). High-crowned or hypsodont teeth are typically associated with grazers; mesodont teeth are typically found in mixed-feeders, whereas brachydont teeth are generally found in browsers (Janis, 1988). This method is widely regarded as one of the most reliable morphological predictors of diet in ungulates (Janis, 1988; Fortelius and Solounias, 2000). In mammoths in particular, there is a tendency of an increase in the hypsodonty index during the Pleistocene, related to the changing environmental conditions of the epoch (Rivals et al., 2019).

Stable Carbon Isotopes: Carbon isotopes analysis can be employed to determine the animal communities that inhabited an area in a specific time frame. Carbon isotopes measured in mammal tooth enamel are a reliable indicator of the animal's diet and metabolic process. For large terrestrial herbivorous mammals (such as proboscideans), the fractionation between carbon isotopes in their food (plants) and tooth enamel is approximately 14‰ (Cerling et al., 1999). Plants can be classified into specific isotopic categories due to metabolic differences, with the most significant ones being plants that utilize the C_3 or C_4 photosynthetic pathway (Teeri and Stowe, 1976). C_3 plants, which include cool-season grasses, trees, and shrubs, exhibit a carbon isotopic value of around −25‰. On the other hand, C_4 plants, typically found in dry environments, have carbon values around −12‰ (Drucker et al., 2015).

The stable carbon isotope method relies on the fact that C_4 plants (grasses and sedges) accumulate a higher proportion of the heavier ^{13}C isotope during CO_2 fixation compared to C_3 plants (e.g., trees, shrubs, and bushes). As a result, C_4 consumers (grazers) show higher levels of ^{13}C in their teeth and bones compared to C_3 feeders (browsers). Animals that consume a mix of C_3 and C_4 vegetation display variable ^{13}C values falling between the ranges of browsers and grazers (Lee-Thorp et al., 1989). While stable isotope analysis is a valuable tool for determining whether an animal was a C_4 grazer, C_3 consumer, or a mixture of both, it has limited ability to discriminate dietary preferences, such as distinguishing between a C_3 browser and a C_3 grazer (Higgins, 2018).

Dental microwear: Dental microwear analysis provides dietary information regarding the last weeks or even days before the death of the animal, thus offering a detailed snapshot of the palaeoenvironment for a very specific period of time, while simultaneously allowing scientists to draw useful conclusions concerning seasonal dietary adjustments of the animal's diet (Rivals et al., 2019). Microwear analysis examines microscopic wear patterns, in the form of pits and scratches, produced on the enamel by food particles (phytoliths present in the leaves, grasses, or fruit and seed coats) and grit or dust present on the surface of vegetation (Solounias and Semprebon, 2002; Lucas et al., 2013). Based on the average number of pits and scratches, the method classifies animals into browsers (that feed on relatively soft, woody and non-woody dicotyledonous plants), grazers (diet that includes mostly grass) and mixed-feeders (combination of the two categories) (Rivals et al., 2011). Browsers tend to have more pits, whereas grazers tend to have more scratches; mixed feeders alternate seasonally between browsing (low pattern scratches) and grazing (high pattern scratches), and therefore the scratches they show on their teeth take on intermediate values, with a slight overlap with the correlating values of browsers or grazers depending on the diet of the organism in the last period of its life (Rivals et al., 2011). Mixed-feeders seem to be more flexible on their dietary plan, being able to consume both grasses and softer plant segments and alternate their diet at will, depending on various environmental factors such as the scarcity of certain plants and grass or the seizure of certain ecological margins by other species, proboscideans or not (Saarinen et al., 2015).

Dental mesowear: This method refers to both the shape and the macroscopic relief of worn molar surfaces (Saarinen et al., 2015) and serves as a proxy for the relative amount of abrasive plant material (mainly grass) eaten by herbivorous mammals (Fortelius and Solounias, 2000). Occlusion during mastication causes the tooth enamel to wear down proportionally to the overall grittiness of the individual’s diet (Saarinen et al., 2015).

Originally, the mesowear method developed by Fortelius and Solounias (2000) studied the dental wear (both abrasive and attritive) of mammals with selenodont dentition, through macroscopic examination of the worn cusps’ apices. However, the much different morphology of proboscidean molars as well as the differences in the way that these mammals tend to chew, produce different wearing patterns (Saarinen et al., 2015). For this very reason, Saarinen et al. (2015) introduced the dental mesowear angle method, which evaluates the worn chewing surfaces by measuring the angles that are formed between the enamel ridges and the dentine valley within the lamella, shown to be related to specific dietary preferences. Specifically, C_4 grass vegetation is heavily abrasive and causes equal rates of wear (regarding both degree and intensity) on enamel and dentine, producing larger mesowear angles and relatively flat occlusal relief (Saarinen et al., 2015). The reason why such plant material in particular causes abrasion-dominated mesowear on molar surfaces is still debated but is most likely due to factors such as the high fiber and phytolith content of grass leaves or extrinsic elements such as sand and dust particles (Lucas et al., 2012). On the other hand, softer plant material (C_3 vegetation) favors tooth-on-tooth abrasion, which accelerates dentine wear, making it occur faster than enamel wear (which is harder). This dietary preference is associated with smaller mesowear angle values and uneven occlusal surfaces, with deeper dentine valleys (Saarinen et al., 2015).

Like microwear analysis, mesowear angle analysis is used to distinguish “browsers” from “grazers” and their intermediate category, “mixed-feeders”. When the mesowear angle is above 117°, proboscideans fall into the grazing category indicating that >90% of their diet is comprised of C_4 grasses. Mean mesowear angles between 106° and 117° classify the proboscideans as mixed-feeders. Lastly, mean mesowear angles below 106° designate them as browsers, implying a diet that consists of >90% soft leaves, bushes, and fruits (Saarinen et al., 2015, and modifications in Saarinen and Lister, 2023). The consistency of this method is based on the predictable wear rate of elephant molars that feed on a particular spectrum of vegetal resources (Saarinen et al., 2015).

In contrast to dental microwear analysis, dental mesowear can be applied relatively easily and in a short time frame (even for a large sample of molars) because it requires a rather simple angle measurement in the lamellae of a molar, using a digital angle meter or a contour gauge. Moreover, because mesowear analysis requires a significant amount of wear to have been developed on the molar (a procedure that can last for years), it depicts the elephants’ dietary preferences on a considerably longer temporal scale than microwear (Rivals et al., 2010). As such, the combination of dental micro- and mesowear methods can provide precise results for a safe interpretation of the diet of a mammal (and consequently of the studied areas’ palaeoenvironment), thus allowing the differentiation of short-term (seasonal) and long-term (average annual) diets (Rivals and Semprebon, 2006).

2. Scope of study

The present study aims to conduct a comprehensive dental mesowear angle analysis on proboscidean molars from several Pliocene–Pleistocene localities in northern and southern Greece, in order to illuminate the dietary habits and ecological adaptations of the Greek proboscideans during the studied period. The ultimate goal of this research is to provide valuable insights into the palaeoecology and evolutionary dynamics of proboscideans, correlating dental wear with environmental conditions and possible dietary shifts. In order to secure the taxonomic attributions of the examined specimens, particularly those belonging to the older collections of LGPUT, before applying the mesowear analysis, an updated taxonomic review is provided including brief descriptions and basic metrical comparisons of the specimens.

3. Materials and methods – Fossiliferous localities

3.1. Material and Methods

The material examined for the mesowear angle analysis consists of molars (m1-m3 refer to the lower molars, while M1-M3 refer to the upper ones) belonging to *M. rumanus*, *M. meridionalis*, *M. trogontherii* and *P. antiquus* originating from various Pliocene–Pleistocene localities of Greece. Most of the specimens are housed at LGPUT, but several ones are stored at AMPG, EPS, HPCS, and PHP.

Dental terminology used for the description of the specimens follows Todd (2010). Dental measurements were taken after Lister and Sher (2015) with a digital caliper. Measurements include length (L), width (W), enamel thickness (ET), lamellar frequency (LF) and plate number (PN). Due to the fragmented nature of the majority of studied specimens, the "length" parameter was not utilized for the species attribution. Comparative measurements were taken from Maglio (1973), Lister et al. (2012), Konidaris et al. (2020), and Lister (2022). The dental-wear-based age criteria for the extant African savannah elephant *Loxodonta africana* provided by Laws (1966) were applied on each specimen.

For the dental mesowear angle analysis, the methodology of Saarinen et al. (2015) was employed. Specifically, mesowear angles were measured on the occlusal surface of each molar's lamellae (Fig. 4), by placing the contour vertically on the occlusal surface of each selected lamella and pressing it against the surface of the tooth that was in wear, along the lingual half of the molar (not along the widest part of the lamellae in the center of the molar). As a result, the lamellae's valleys were distinctively portrayed on top of the contour gauge as angles. To obtain the most representative measurements possible, the angles from the three central complete enamel loops of each specimen were calculated (with the exception of two *M. meridionalis* from Tsotylion where worn enamel rings were measured to increase the available sample). The mesial-most or distal-most enamel bands were avoided, as these are often too worn or not worn enough, respectively, for mesowear analysis (Saarinen et al., 2015). The angles were then photographed separately from the tooth, using a camera stand to prevent parallax error. Teeth and contour gauge were photographed using the same camera settings for each photograph. The contour gauge images were edited using the software Inkscape and then digitally measured and analyzed using ImageJ software (Abramoff et al., 2004; https://imagej.net/ij/). Then the mean angle was calculated by averaging the three measurements of each specimen. For mandibles and maxillas, bearing both left and right molars (e.g., m3 sin and m3 dex), the average angle value of the two was used. Similarly, for crania featuring four molars (e.g. m3 sin, m3 dex, M3 sin and M3 dex) we used the average of the four mean mesowear angle value measurements to represent the individual. In the case of fragmentary or badly preserved molars, a minimum of two central lamellae was used for calculating the mesowear angle. Finally, the results were compared to the corresponding angle ranges of Saarinen et al. (2015) and Saarinen and Lister (2023), classifying each individual to the three main dietary categories: browsers (<106°), mixed feeders (106–117°) and grazers (>117°).

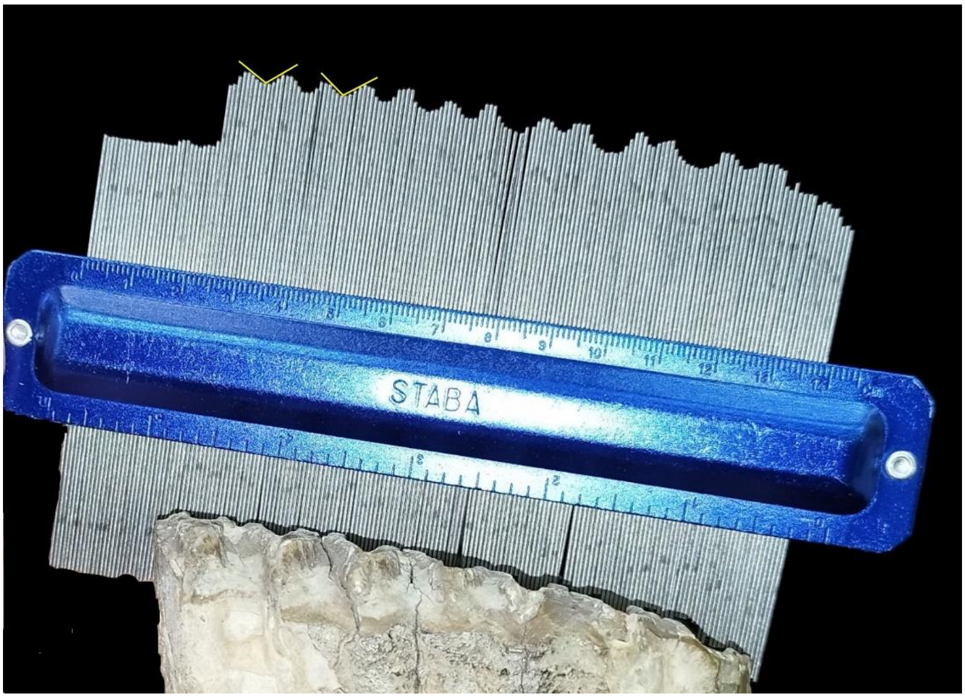

Figure 4. Measuring of the mesowear angles with the use of a contour gauge.

The results of the mesowear analysis were statistically compared using two methods. For localities featuring only one or two specimens, the z-score was computed as $z = (x - m) / SD$, where x is the mean mesowear angle of the examined specimen, and m and SD, the mean value and standard deviation of the comparative sample (with ≥3 specimens), respectively. In localities with three or more specimens available, the pairwise Mann-Whitney test was applied, comparing the mean mesowear angles of the specimens. Box-and-whisker plots and statistical computations were performed with PAST v. 4.04 (Hammer et al., 2001; https://www.nhm.uio.no/english/research/resources/past/).

3.2 Abbreviations

AMPG, Museum of Palaeontology and Geology, National and Kapodistrian University of Athens, Greece; **EPS**, Ephorate of Paleoanthropology – Speleology, Athens, Greece; **HPCS**, Historical Palaeontological Collection of Siatista, Trampantzeion; **LGPUT**, Museum of Geology-Palaeontology-Palaeoanthropology of the Laboratory of Geology and Palaeontology, Aristotle University of Thessaloniki, Greece; **PHP**, Palaeontological and Historical Museum of Ptolemaida.

3.3 Fossiliferous localities

Figure 5. Map of Greece with the fossiliferous localities documenting the herein studied Pliocene–Pleistocene proboscideans. **1**, Philippi (*M. meridionalis*, *M. trogontherii*, *P. antiquus*); **2**, Symvoli (*M. meridionalis*); **3**, Apollonia-1 (*M. meridionalis*); **4**, Sotiras (*M. trogontherii*); **5**, Amyntaio (*P. antiquus*); **6**, Pentavrysos (*P. antiquus*); **7**, Siatista (*P. antiquus*); **8,** Tsotylion *(M. rumanus, M. meridionalis*, *P. antiquus*); **9**, Kapetanios (*M. meridionalis*); **10**, Polylakkos (*M.* cf. *rumanus*); **11**, Loussika (*M. trogontherii*); **12**, Roupaki (*P. antiquus*); **13,** various localities in the Megalopolis Basin, including Marathousa 1, Kyparissia 3 and the localities excavated by T. Skouphos and J. Melentis. Image exported from Copernicus Land Monitoring Service, https://land.copernicus.eu/

Apollonia-1 (APL): APL is located in proximity to the village of Nea Apollonia, roughly 45 km east of Thessaloniki, and was discovered in 1990 (Koufos et al., 1992). APL is situated in the Mygdonia Basin, which represents an east–west-trending tectonic depression in Central Macedonia (Fig. 5). The Pre-Mygdonian Group of the sedimentary sequence of the basin includes the Chryssavgi Formation (Fm), the Gerakarou Fm and the Platanochori Fm (Koufos et al., 1995). APL belongs to the latter Formation, which consists of sands, sandstones, conglomerates, silty sands, silts, clays, marls, and marly limestones, indicating the presence of small lakes and swamps (Koufos et al., 1995). The site has provided a diversified fauna rich in horses, bisons, deer, and carnivorans (Koufos and Kostopoulos, 2016). Based on mammal biochronology the APL fauna is dated at the end of the late Villafranchian/Epivillafranchian (Lower Pleistocene), between ca. 1.5 and 1.2 Ma (Koufos and Kostopoulos, 2016; Konidaris et al., 2020). Further information on the stratigraphy of the Mygdonia Basin and the fauna of APL is provided in Koufos et al. (1995), Konidaris et al. (2015), and Koufos and Kostopoulos (2016).

Loussika: The site is located in NW Peloponnese (Fig. 5), in the valley of the small stream Serdini, a tributary of the primary river Peiros. The fossiliferous deposits are of low-energy fluvial origin and consist of clayey sand, sand, and coarse sand (Athanassiou, 2012). At Loussika, a partial skeleton of *M. trogontherii* was excavated in 2001 and 2003 and studied by Athanassiou (2012), who proposed an early Middle Pleistocene age for the site. Further details on the site and the mammoth skeleton are provided in Athanassiou (2012).

Megalopolis Basin: The Megalopolis Basin, located in central Peloponnese (Fig. 5) is a tectonic, post-orogenic half-graben filled with Neogene to Holocene continental sediments (Vinken, 1965). The Neogene sedimentary sequence of the basin consists of the Pliocene Makrision and Trilofon Fm, and the Pleistocene Apiditsa, Choremi and Potamia/Thoknia Fm (e.g., van Vugt et al., 2000). The herein examined specimens originate from the Choremi Fm, which is further divided into the lower Marathousa Member (Mb) and the overlying Megalopolis Mb (van Vugt et al., 2000). During the late Early Pleistocene and the Middle Pleistocene (ca. 900 to 150 ka), the basin hosted a large and shallow lake, which resulted in a sedimentary sequence composed mainly of lacustrine sediments intercalated by lignite seams (Vinken, 1965; van Vugt et al., 2000; Tourloukis et al., 2018a).

The first systematic palaeontological excavations took place by Prof. Th. Skouphos in 1902 and the material was studied in detail in a series of articles in the 1960s by Prof. I. Melentis. Among this first collected material, proboscideans comprised an important part and were studied by Melentis (1961, 1963). As part of a historical collection, this material lacks precise stratigraphic control, but is assumed to originate at its most part from a region near the Isoma Karyon village and can be roughly dated to the late Middle–Late Pleistocene (Athanassiou, 2022). Melentis (1961) attributed the material to several proboscidean taxa, however, all of it belongs to *Palaeoloxodon antiquus* (see Athanassiou, 2022). Later on, Melentis (1965) excavated a cranium of *P. antiquus* from Lefktro, enriching further the Megalopolis collection. All this material is hosted at AMPG and was examined in the present thesis; it is here referred to as “Megalopolis (old collection)”.

Recent research in the basin (e.g., Athanassiou, 2018; Athanassiou et al., 2018; Panagopoulou et al., 2015, 2018; ongoing studies) resulted in the discovery of several new sites that significantly enriched the Megalopolis Basin faunal material. Among the new collected material several proboscidean specimens (including partial skeletons) were discovered, and the molar sample is examined in this thesis. This includes molars from the sites Kyparissia 3 (KYP-3) and Marathousa 1 (MAR-1). Kyparissia 3 is located below Lignite II of the basin (Karkanas et al., accepted) and contains an early Middle Pleistocene fauna (Athanassiou, 2018; Athanassiou et al., 2018). Two molars of *P. antiquus* from this site are included in this thesis, one belonging to a hemimandible that was studied in Athanassiou (2018) and the other, still unpublished, is part of the recent field research in the basin (Karkanas et al., accepted).

Marathousa 1 (MAR-1) is a Middle Pleistocene (Lower Palaeolithic) site, which was discovered in 2013 and excavated until 2019 (Panagopoulou et al., 2015, 2018; Harvati et al., 2018). MAR-1 is radiometrically, magnetostratigraphically, and biochronologically dated to

500–400 ka, and is correlated to the glacial MIS 12 (Tourloukis et al., 2018). MAR-1 is situated between the Lignite Seams IIb and IIIa (Karkanas et al., 2018). It has yielded a stratified archaeological and palaeontological assemblage, the latter including micro- and macrofauna (e.g., ostracods, mollusks, fishes, amphibians, reptiles, birds, mammals), and micro- and macroflora (Doukas et al., 2018; Field et al., 2018; Karkanas et al., 2018; Konidaris et al., 2018; Michailidis et al., 2018; Tourloukis et al., 2018b; Bludau et al., 2021; Boni, 2022). Of particular importance is a partial skeleton of an adult male individual of *P. antiquus* discovered at the site's Area A, preserving evidence of butchering by hominins (Konidaris et al., 2018). The molars of this elephant are examined in the present thesis.

Philippi: The Philippi fossil locality belongs to the Drama minor basin, which is located in eastern Macedonia (Fig. 5), to the east of the Strymonikos major basin. Geotectonically, it belongs to the large rifting basins of the Tertiary, bordered from west to east by the Rhodope massif. More information can be found in Maravelis et al. (2022 and references therein). According to Psarianos (1958) and Marinos (1965), the proboscidean fossils (examined in the present thesis) were collected from the swamp area (tenaghi) of Philippi, located northwest of the city of Kavala. The sediments of this area are primarily Pleistocene and possibly correspond to the last two glacial and interglacial periods (Marinos, 1965). Extensive research in the area indicates that the base of the sedimentary sequence of Tenaghi Philippon extends to 1.35 Ma (Tzedakis et al., 2006).

Another locality situated inside the Drama subbasin, which yielded proboscideans is Symvoli (Melentis, 1966), located near the homonymous village of Serres Prefecture. According to the IGME (Institute of Geology and Mineral Exploration) geological map (Drama Sheet, 1979), the Pleistocene sediments near Symvoli consist of red silts and conglomerates alternating with red sandy clays.

Ptolemais Basin: The Florina–Ptolemais–Servia Basin is a northwest-southeast trending sedimentary basin in NW Greece (Fig. 5). The Neogene of the basin is divided into four lithostratigraphic Formations (Fm): the Upper Miocene Komnina Fm, the Pliocene Ptolemais Fm, and the Pleistocene Proastio and Perdikas Fms (Steenbrink et al., 2006). The lower Pleistocene Proastio Fm consist of conglomerates in alternation with white-gray sands and clays, and the overlying Perdikkas Fm with fluvial-torrential conglomerates, and dark red sands and gravels (Koufos and Pavlides, 1988). From the region of Sotiras the presence of *M.*

trogontherii and *P. antiquus* is already recorded (Velitzelos and Schneider, 1973; Tsoukala et al., 2011). The studied proboscidean material was mostly gathered from local active sand mines and the precise stratigraphic horizon is unknown. The molar from Pentavrysos, stored at PHP lacks also stratigraphic information. However, the hemimandible of *M. trogontherii* from Sotiras (LGPUT-MP-42) was collected from the Proastion Fm (Koufos and Pavlides, 1988), and the *P. antiquus* skeleton (PHP) originates from the Perdikkas Fm (Kevrekidis and Mol, 2016). More information on the geology and the stratigraphy of the basin can be found in Maravelis et al. (2022 and references therein).

Haliakmon river system (Tsotylion, Polylakkos, Siatista): In the area near Tsotylion (NW Greece; Fig. 5) deposits are exposed mainly E–SE of the Tsotylion village and along Pramoritsas river and include Upper Pliocene to Lower Pleistocene sandy deposits of fluvial origin. According to Eltgen (1986) and Fountoulis et al. (2001) the continental deposition in this area started after 3.4 Ma. The wider region has provided abundant fossils most notably in Milia, dated to the early Villafranchian (e.g., Tsoukala and Mol, 2016), but also in different fossil spots (e.g., Libakos, Polylakkos, Kapetanios; Steensma, 1988) with most of the fauna dated to the late Villafranchian (Early Pleistocene). Several mammoth and elephant specimens examined here originate from the area of Tsotylion, but all lack precise stratigraphic information. The maxilla of *M. rumanus* from Tsotylion is considered to originate from the oldest terrestrial deposits, those correlated to the Late Pliocene (Kostopoulos and Koulidou, 2015). The molars from Tsotylion attributed to *M. meridionalis* originate possibly from the Lower Pleistocene deposits (likewise the molar from Kapetanios), whereas the presence of *P. antiquus* from Tsotylion indicates a Middle–Late Pleistocene age. Furthermore, two molars of *M.* cf. *rumanus* are documented as originating from Polylakkos, a locality from where Steensma (1988) notes the presence of *Anancus* yet based only on a femur.

The town of Siatista is located ca. 20 km to the west of Tsotylion (Fig. 5), west of the Haliakmon river. The specimens from the Siatista collection (HPCS), lack precise information regarding their locality and geological age, but are considered to originate from the wider area of Siatista (Mol et al., 2010). The presence in this collection of *Anancus arvernensis*, *Stegodon* sp., *Mammuthus meridionalis* and *Palaeoloxodon antiquus* (Mol et al., 2010) indicates a wide chronological range. Here, molars of *P. antiquus* were examined broadly indicating a Middle–Late Pleistocene age.

4. Systematic palaeontology

Order Proboscidea Illiger, 1811

Family Elephantidae Gray, 1821

Subfamily Elephantinae Gray, 1821

Genus *Mammuthus* Brookes, 1828

***Mammuthus rumanus* (Stefanescu, 1924)**

Locality: Tsotylion, Western Macedonia.

Age: Precise locality and stratigraphic horizon unknown but possibly Late Pliocene.

Material examined: Partial right maxilla with M2 and M3, LGPUT-MP-04.

Figure 6. Ventral view of the *Mammuthus rumanus* right maxilla bearing the M2 and M3 (LGPUT-MP-04) from Tsotylion.

Remarks: The maxilla fragment MP-04 (Fig. 6) was described in detail in Kostopoulos and Koulidou (2015). Taking into consideration the low LF, the thick enamel, and the low hypsodonty index, the specimen was attributed by the authors to *Mammuthus* sp. (primitive Eurasian morph). Here it is included within *M. rumanus* for the sake of simplification. Due to its advanced stage of wear, only the M2 was selected for the mesowear analysis.

Mammuthus* cf. *rumanus

Locality: Polylakkos, Western Macedonia.

Age: Stratigraphic horizon unknown but possibly Late Pliocene.

Material examined: Left m1/m2 fragment, LGPUT-MP-07; right m2/m3 fragment, LGPUT-MP-40.

Description: The mesial part of MP-07 is missing. The molar is parallel-sided with a slight curvature at the distal end, as far as it can be observed from the preserved part (Fig. 7). The greatest width is measured at the crown base. Anterior and posterior columns are present, and there are seven apical digitations at the distal end of the tooth. The lateral sides of the enamel figures are rounded and their direction is even. The enamel figures are symmetrical, both mesiodistally and linguobuccally. The medial area of the figures is looped and the wear results in the contact of the medial edges of the figure. Undulating enamel folding appears mainly in the median area of the tooth.

Figure 7. Occlusal view of the left m1/m2 fragment (LGPUT-MP-07) of *Mammuthus* cf. *rumanus* from Polylakkos.

The mesial and distal parts of MP-40 are missing. The tooth is parallel-sided and its greatest width can be observed in the middle of the distance between the crown base and the occlusal surface. The lateral edges are high and slightly bowed out. On the occlusal surface, the fragmented nature of the specimen does not allow safe conclusions about the apical digitations. The enamel figure is parallel sided with a median loop at the first preserved lamella, while the lateral sides are rounded and even. The medial edges are separated and the folds are places throughout the length of the enamel figure. The enamel folding is regular.

Figure 8. Occlusal view of the right m2/m3 fragment (LGPUT-MP-40) of *Mammuthus* cf. *rumanus* from Polylakkos.

Remarks: MP-07 was originally described in Psarianos (1958) and was attributed to "*Archidiskodon*" cf. *meridionalis*, while later Koulidou (2013) assigned it to *Mammuthus* cf. *rumanus*. Taking into consideration primitive traits such as the increased ET and the loosely spaced lamellae (low LF), outside the range of *M. meridionalis* given by Maglio (1973; App. Table 2), the specimen is indeed closer to *M. rumanus.* Given its fragmented nature, the molar is tentatively attributed to either m1 or m2, due to the lack of tapering in the posterior end.

Similarly, MP-40, has also primitive traits such as high ET and low LF values (App. Table 1), which fall outside the range of *M. meridionalis* m2. Given the lack of data regarding *M. rumanus* m2, and the relatively small width of the specimen, MP-40 is identified here as either a m2 or a m3. For the purpose of mesowear angle analysis both the above specimens are treated as *M.* cf *rumanus*.

***Mammuthus meridionalis* (Nesti, 1825)**

Locality: Tsotylion, Western Macedonia.

Age: Precise locality and stratigraphic horizon unknown (Early Pleistocene based on the presence of *M. meridionalis*).

Material examined: Left M3 fragment, LGPUT-MP-16; left m2 fragment, LGPUT-MP-17; right m2 fragment, LGPUT-MP-43 (previously labeled as MP-Y).

Description: MP-16 is identified as a M3 due to the tapering at its distal part (Fig. 9). Most of the mesial part of the molar is missing and preserved are eight plates and the distal talon, five of which are worn and in use. There are more than five apical digitations and there is no complete enamel loop. There is no visible plate inclination. The enamel figure shape is parallel-sided, with the median area being open. The lateral sides are rounded and evenly directed. The medial edges are separated. Enamel folding is absent to irregular and spread throughout the length of the loop. The folding of the enamel is low and the spacing between the folds is loose. Molar roots are present, developed and the S curve can be observed at the lateral sides of the molar.

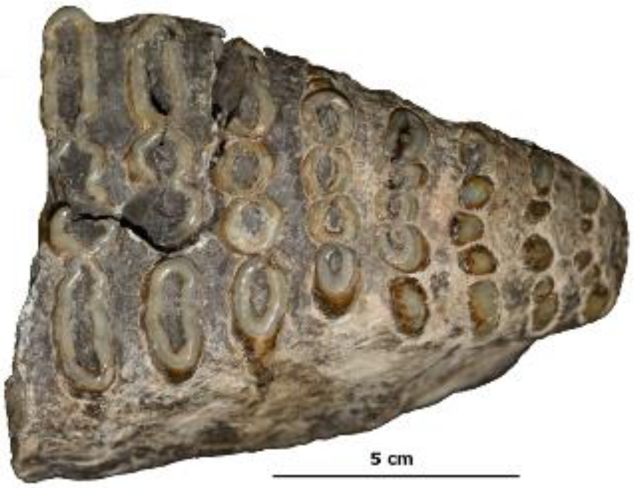

Figure 9. Occlusal view of left M3 fragment (LGPUT-MP-16) of *Mammuthus meridionalis* from Tsotylion.

MP-17 is a fragmented m2 (Fig. 10). A mesial talon and six plates are preserved, the five of them in wear. No complete enamel loop is formed. The molar is parallel-sided with a slight curvature. Its greatest width is present at the occlusal surface. The occlusal surface is even, and the plate inclination weak. The enamel figure shape is parallel-sided. Both lateral and longitudinal sides are rounded, and the direction of the former is even. The enamel figure is asymmetrical, while the medial edges of the enamel loops are separated with reasonable distance between them. The enamel folding is irregular and the folds are spread in all the molar length. Strong posterior columns are present from the second to the fourth lamella.

Figure 10. Occlusal view of the left m2 fragment (LGPUT-MP-17) of *Mammuthus meridionalis* from Tsotylion.

The m2 MP-43 is missing its mesial part and preserves nine plates, five of which are in wear (Fig. 11). There is slight curvature, and its height is even at both ends. The greatest tooth width appears at half-crown-height. There is no S curve and the lamellae are parallel sided. The lateral edges of the plate are high and slightly bowed out. There are few apical digitations and the appearance of the first complete enamel loop is slow (within six worn plates). There is no cingulum in the distal end. The roots are not preserved. The enamel figure shape is elliptic and parallel sided, with the median area folded and the lateral sides rectangular and even (not directed towards the mesial or the distal end). The enamel figures are symmetrical, both mesiodistally and linguobuccally. Its medial edges are in contact, with a noteworthy gap between them. Enamel folding is irregular and it is spread throughout the entire length of the enamel figure, while having low amplitude.

Figure 11. Occlusal view of the right m2 fragment (LGPUT-MP-43) of *Mammuthus meridionalis* from Tsotylion.

Remarks: MP-16 was first described by Koulidou (2013) and attributed to *M.* cf. *trogontherii*, based on the W/LF value, which indeed exceeds slightly the *M. meridionalis* upper limit. However, taking into consideration the rather thick enamel (3.4 mm) and the high occlusal angle of 130° (the angle that is formed between the tangent lines on the worn and unworn occlusal surfaces of the molar in lateral view) that exceeds the upper limit known from *M. trogontherii* from Süßenborn (see Konidaris et al., 2020: fig. 7, and references therein), it probably belongs instead to *M. meridionalis*, a species already present at Tsotylion.

The morphological and metric traits of MP-43 (App. Table 2) allow for an attribution to *M. meridionalis*, in line with its original attribution by Psarianos (1958).

MP-17 was firstly described by Koulidou (2013) and attributed to *M. meridionalis*. Indeed W, LF and ET are within the known range of *M. meridionalis* (App. Table 2) and support the allocation to this species.

Locality: Philippi, Drama Basin, Eastern Macedonia.

Age: Precise locality and stratigraphic horizon unknown (Early Pleistocene based on the presence of *M. meridionalis*).

Material examined: Right m3 fragment, LGPUT-MP-18; left m3 fragment, LGPUT-MP-30.

Description: A significant part of MP-18 is missing and only four worn plates from the middle part of the tooth are preserved (Fig. 12). The molar is widest in the middle. The lateral edges of the plates appear high and slightly bowed out in the middle. The enamel figure is parallel-sided with a median loop and its lateral sides are rounded and turned towards the anterior end. In addition, there is a significant gap between the loops and as a result their median edges are not in contact with each other. The figures are asymmetrical with regard to the long axis of the molar. The enamel folding is strong with crinkled form, and present throughout the enamel figure. In lateral view, the plates are S-shaped.

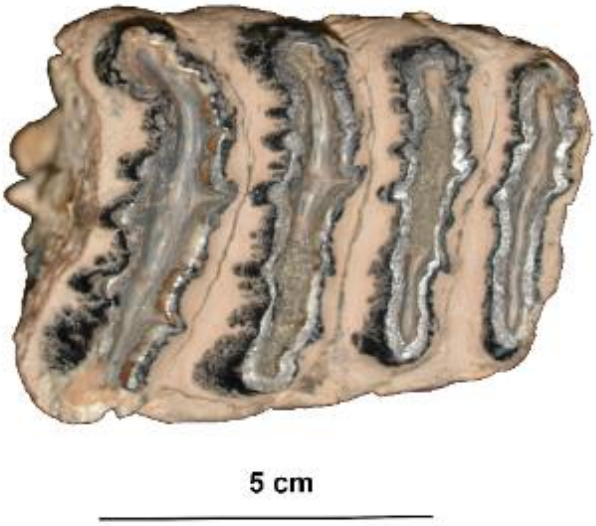

Figure 12. Occlusal view of the right m3 molar fragment (LGPUT-MP-18) of *Mammuthus meridionalis* from Philippi.

MP-30: Only the five lamellae (the distal two of which are less worn) of MP-30 are preserved (Fig. 13). The lateral edges of the plates are high and bowed out. The molar roots are visible and open. The maximum width appears on the crown. A few apical digitations are visible, and the first completed enamel appears relatively quickly, within three worn plates. The enamel figure shape can be characterized as pseudo-lozenge, and the median area is folded. The lateral sides of the enamel figures are rounded. The enamel figure appear symmetrical, both mesiodistally and linguobuccally.

Figure 13. Occlusal view of the left m3 fragment (LGPUT-MP-30) of *Mammuthus meridionalis* from Phillipi.

Remarks: Koulidou (2013) identified both MP-18 and MP-30 as either m2 or m3 due to their fragmented nature. Judging from the metrical and morphological traits the MP-18 is closer to a m3 and is tentatively treated as such. Moreover, because the distal end of MP-30 is preserved, the marked tapering indicates also in this case an attribution to m3. Regarding their taxonomy, ET, LF and W values of both specimens fall between the ranges for *M. meridionalis* lower m3, given by Maglio (1973).

Locality: Symvoli (Drama Basin).

Age: Precise locality and stratigraphic horizon unknown (Early Pleistocene based on the presence of *M. meridionalis*).

Material examined: Left M3, AMPG-1964/449.

Figure 14. Occlusal view of the left M3 (AMPG-1964/449) of *Mammuthus meridionalis* from Symvoli.

Remarks: This molar was originally described by Melentis (1966) and was attributed to the new subspecies "*Archidiskodon meridionalis proarchaicus*" based on its low LF and thick enamel. Athanassiou (2022) notes that this molar exhibits morphological and metrical similarities to already published samples of *M. meridionalis*, therefore lacking distinctive features that would allow for a distinction at subspecific level, rendering *A. m. proarchaicus* synonymous to *M. meridionalis*.

Locality: Kapetanios, Western Macedonia.

Age: Early Pleistocene.

Material examined: Right m3, LGPUT-KAP-1.

Description: The mesial part of KAP-1 is missing (Fig. 15). It tapers distally and its occlusal surface is generally ovated with a slight curvature at the posterior end. The greatest width is met at the upper half of the crown. The inclination of the plates to the occlusal surface is rather weak. The lateral edges of the plate are mesiodistally short and rounded. The molar roots are not preserved . The first enamel loops appear progressively, after eight worn plates, while there are also four apical digitations. The median area of the enamel loop is folded, while the lateral are evenly rounded, with no distinct direction either distally or mesially. The enamel figures are symmetrical, both mesiodistally and linguobuccally, while the medial edges of enamel are separated. The enamel folding is irregular with the folds present only in the median area of the loop.

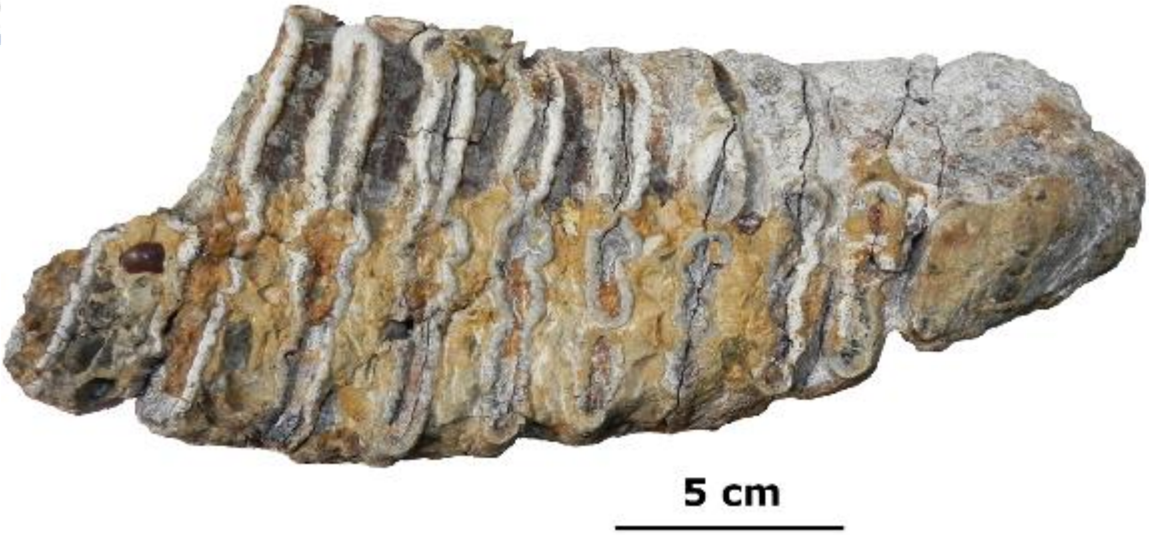

Figure 15. Occlusal view of the right m3 fragment (LGPUT-KAP-1) of *Mammuthus meridionalis* from Kapetanios.

Remarks: This molar was studied by Steensma (1988) who based his attribution on the metrical similarities between the KAP-1 and the values provided by Maglio (1973) for the typical *M. meridionalis* from Upper Valdarno (Italy). This attribution is followed also here. Despite that it was originally identified as a left m3 (Steensma, 1988), based on the curvature it is identified here as a right one.

Locality: Apollonia 1, Mygdonia Basin, Central Macedonia.

Age: Late Villafranchian/Epivillafranchian, Early Pleistocene.

Material examined: Left M3 fragment, LGPUT-APL-686B; right hemi-mandible with m3, LGPUT-APL-716; left m3, LGPUT-APL-687.

Remarks: The APL specimens were described by Konidaris et al. (2020). Mandibular and dental traits permit their attribution to *M. meridionalis*. Based on the presence of more advanced features compared to the typical *M. m. meridionalis* from Upper Valdarno, the material was assigned to *M. m. vestinus*.

Mammuthus trogontherii **(Pohlig, 1885)**

Locality: Sotiras, Ptolemais Basin, Western Macedonia.

Material examined: Right M2 fragment, LGPUT-MP-45 (previously labeled as MP-SOT-S); left m3, LGPUT-MP-46 (previously labeled as MP-SOT-6); left hemimandible with m2, LGPUT-MP-42 (previously labeled as MP-diadrsin); mandible with right and left m2, LGPUT-MP-05; right m3, LGPUT-MP-44 (previously labeled as MP-SOT-Z).

Age: Middle Pleistocene based on the presence of *M. trogontherii*; MP-42 originates from the Proastio Fm of the Ptolemais Basin; for the other molars the precise locality and stratigraphic horizon are unknown**.**

Description: The hemimandible MP-42 bears the complete m2 (Fig. 16). The molar shape is parallel-sided, with a weak curvature at its distal end. The height is even at both ends. The greatest width of the molar is observed at 1/2 up from the base of crown. The plate inclination is weak. There is a small number of apical digitations, resulting in an early appearance of the first complete enamel loop. The lamellae are separated and are intensely folded throughout the entire length of the enamel figures. The latter are parallel-sided with the lateral sides turned mesially.

Figure 16. Dorsal view of the left hemimandible bearing the m2 and the erupting m3 (LGPUT-MP-42) of *Mammuthus trogontherii* from Sotiras.

MP-45 is an almost completely preserved and moderately worn M2. The molar is fragmented with the distal end missing. The dental formula is x9-, with all plates in wear. The shape of the molar is parallel-sided with symmetrical margins and a slight curvature at the distal end. The height is even at both ends. There is strong inclination between the enamel plates and the occlusal surface. The roots are present and are strong. A few apical digitations are present (most likely less than four) and complete enamel loops appear relatively late, between six–seven worn plates. The enamel appears at a noticeable height above the cement. The shape of the enamel figure is parallel-sided with lozenge shaped, separated median loops. The lateral sides of the enamel figures are rectangular while their direction is mostly even, while there are loops that turn both mesially and distally. The enamel figure is symmetrical. The enamel folding is weak, tightly spaced, undulated and present throughout the length of the loops.

Figure 17. Occlusal view of the right M2 fragment (LGPUT-MP-45) of *Mammuthus trogontherii* from Sotiras.

The MP-46 m3 preserves 16 plates, 10 of which are in wear. It is parallel-sided with slight curvature and even height at both ends. The greatest tooth width is observed at the crown. There is strong plate inclination. The lateral edges of each plate are parallel sided. The roots are not preserved. There are many apical digitations, while the first complete enamel loop appears slowly. The S curve of the plates is vivid. The enamel figure shape is parallel sided with folded median area and rounded lateral sides. The lateral sides are even, with a slight curve towards the mesial end, while the median edges are separated. The folding is weak, loosely-spaced, but regular and extending at the entire loop.

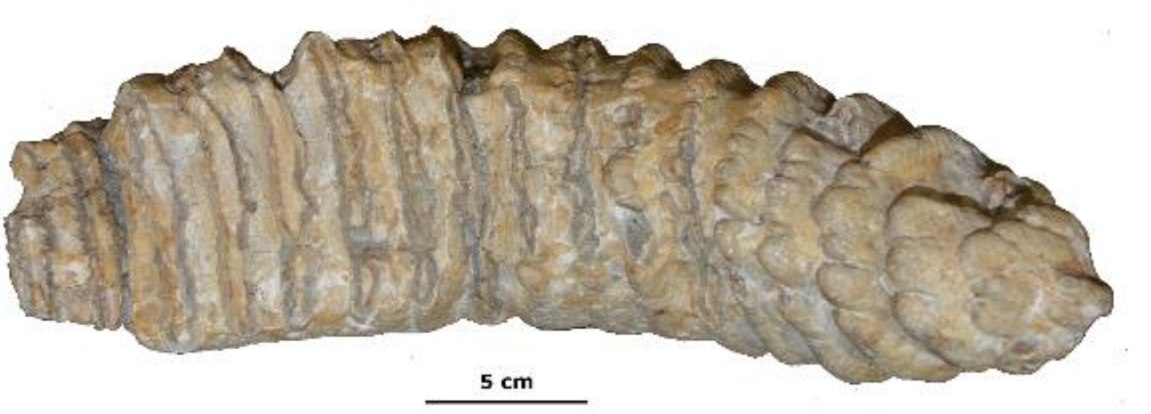

Figure 18. Occlusal view of the left m3 (LGPUT-MP-46) of *Mammuthus trogontherii* from Sotiras.

Both m2 of the mandible MP-05 are heavily worn. They are parallel-shaped with slight curvature. The lateral edges of the plates are high and slightly bowed out. There are no apical digitations visible in any of the molars. The enamel figure is parallel-shaped, with the median area folded and the lateral sides rounded and turned mesially. The medial edges of the enamel loops are in contact in some areas of the tooth due to the intense folding, which appears through the entire length of the loops. The enamel is relatively thin.

Figure 19. Dorsal view of the mandible with the left and right m2 and the erupting m3 (LGPUT-MP-05) of *Mammuthus trogontherii* from Sotiras.

The molar MP-44 lacks its mesial part and preserves ten plates, all in wear. The shape of the tooth is elliptic with the widest part in the middle of its length. There is slight to no curvature in the molar. The greatest tooth width appears at the molar crown. The lateral edges of the plate are high and slightly bowed out. The molar roots are open. There are few apical digitations in each plate and the first complete enamel loops appears quickly (within four worn plates). There is a single column at the posterior end of the molar. The shape of the enamel figure is parallel-sided, with the median area slightly folded. The lateral sides are rounded and turned mesially. The enamel figures are separated. The enamel folding is irregular with the folds spread throughout the entire length of the enamel figure and not only in the medial part.

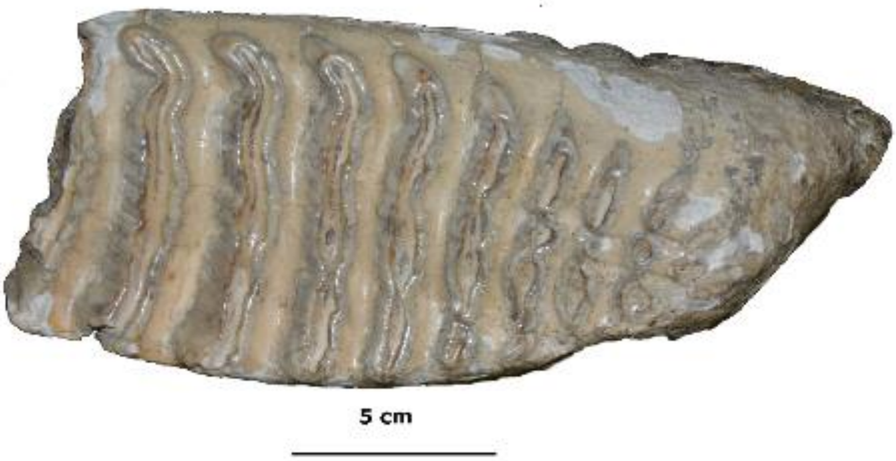

Figure 20. Occlusal view of the right m3 (LGPUT-MP-44) of *Mammuthus trogontherii* from Sotiras.

Remarks: MP-42 was firstly reported as *Mammuthus* cf. *meridionalis* by Koufos and Pavlides (1986) and was later attributed to *M. trogontherii* by Koulidou (2013). Indeed, given that W, ET and LF values fall within the range of *M. trogontherii* m2 from Süßenborn (App. Table 2), it is attributed to this species.

All available measurements (W, ET, LF) for MP-45 (App. Table 1) are in agreement with the attribution to *M. trogontherii* by Koulidou (2013). Specifically, the LF value (6.46) differentiates it from both *M. meridionalis* (the upper limit of LF is 5.7 for M2) and *M. primigenius* (lower limit of LF is 7.7 for M2).

In MP-46, W, ET and LF fall within the ranges of both *M. meridionalis* and *M. trogontherii*, with the PN being the decisive parameter. More specifically, the 18 plates present on the occlusal surface exceed the upper limit of the m3 for *M. meridionalis*, permitting an attribution to *M. trogontherii*.

MP-05 was originally attributed to *P. antiquus* from Koulidou (2013). However, the high W and LF values of the specimen (App. Table 1), fall outside of the corresponding *P. antiquus* ranges, while aligning more closely to *M. trogontherii*. Moreover, the presence of the medial mental foramina (MMF) in the lingual side of both hemimandibles (for this character see Ferretti and De Bryne, 2011), providing further evidence to the new classification.

Similarly, MP-44 was originally attributed to *P. antiquus*. The molar is characterized by increased width exceeding the upper limit of the m3 of *P. antiquus* but within the range of *M. trogontherii* m3, a species already found at Sotiras. Neither MP-44 nor MP-05 bear pointed midline sinuses or the «dot-dash-dot» wear pattern of the distal end enamel rings, both distinctive characteristics of *P. antiquus*.

Locality: Philippi, Drama basin, Eastern Macedonia.

Age: Middle Pleistocene based on the presence of *M. trogontherii*.

Material examined: Left m3, LGPUT-MP-21; right m3, LGPUT-MP-22.

Description: The shape of the m2 MP-21 is elliptic and rather straight, with the widest part appearing at the medial of the molar (Fig. 21). Its greatest width appears at the crown. The plates show strong inclination to the occlusal surface. The lateral edges of the plates are parallel-sided. The molar roots are visible and strong. Five apical digitations are present at the distal part of the molar and the first complete enamel loop appears rather late. The enamel height above the cement is high. The shape of the enamel figures is parallel-sided with the median part being looped. The lateral sides of each plate are rectangular and slightly mesially directed. Despite the enamel figure’s looped shape, the median edges are separated. The enamel folding is crinkled, loose, and present throughout the entire length of the enamel figure.

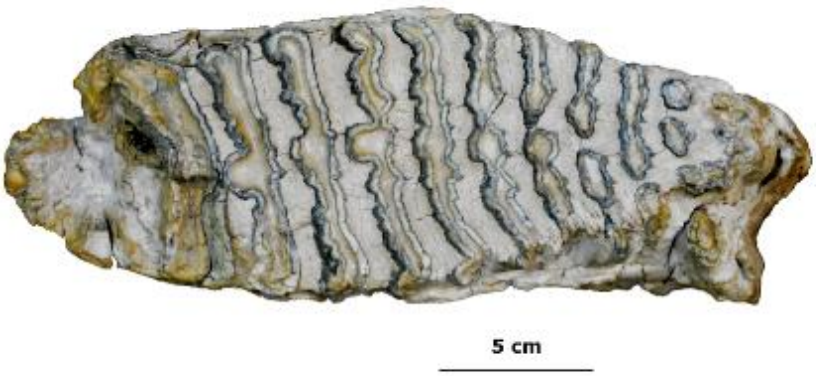

Figure 21. Occlusal view of the left m3 fragment (LGPUT-MP-21) of *Mammuthus trogontherii* from Philippi.

The m3 MP-22 is almost completely preserved (Fig. 22). The molar shape is parallel-sided with symmetrical margins and slight curvature at the distal end. The height is even at both mesial and distal ends. The inclination between the enamel plates and the occlusal surface is strong. The molar roots are present and strong. The distal end of the tooth is partly preserved, but there are a few apical digitations (most likely less than four) and the complete enamel loops appear relatively late, between six to seven worn plates. The enamel appears at a noticeable height above the cement. The shape of the enamel figures is parallel-sided with lozenge shaped and separated median loops. The lateral sides of the enamel figures are rectangular and mostly even but some turn both mesially and distally. The figures are symmetrical. The enamel folding is weak, undulating, tightly spaced and present throughout the loop's length.

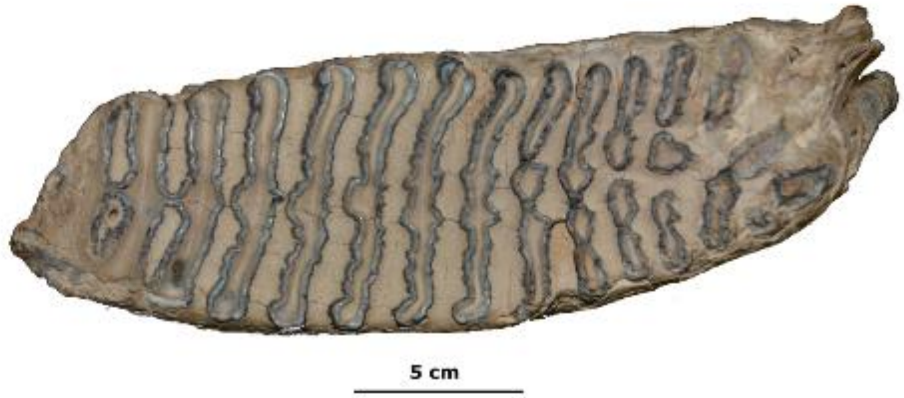

Figure 22. Occlusal view of the right m3 (LGPUT-MP-22) of *Mammuthus trogontherii* from Philippi.

Remarks: MP-21 was first described by Psarianos (1958), while MP-22 was first described by Marinos (1965). Both specimens were attributed to *M. trogontherii*. Indeed, W, LF and ET fall within the ranges for *M. trogontherii* m3 and support the attribution to this species.

Locality: Loussika, northwestern Peloponnese.

Age: early Middle Pleistocene.

Material examined: Cranium with left and right M3 and associated mandible with left and right m2 and m3.

Remarks: The cranium and the mandible belong to a partial skeleton of *M. trogontherii*, described in detail by Athanassiou (2012). The latter author based on the dental similarities of the Loussika mammoth with *M. trogontherii* from its type locality Süßenborn (Germany), proposed an early Middle Pleistocene age for the site. Due to the partial preparation of the cranium at the time of the measurement, mesowear angle was taken only from the left upper molar; both lower third molars were measured.

Genus *Palaeoloxodon* (Matsumoto, 1924)

Palaeoloxodon antiquus (Falconer and Cautley, 1847)

Locality: Tsotylion, Western Macedonia.

Age: Precise locality and stratigraphic horizon unknown (Middle–Late Pleistocene based on the presence of *P. antiquus*).

Material examined: Mandible with left and right m2, left M2 and right M2; LGPUT-MP-02.

Description: All four molars of MP-02 are parallel-sided, with slight curvature towards the distal end, and strong plate inclination. The first appearance of complete enamel loops is rather quick (within three worn plates in all molars). The enamel figure shape is parallel-sided with the characteristic pointed midline sinuses. The lateral sides are rounded, while the medial edges are separated. Enamel folding is strong, crinkled and spread throughout the enamel figure length. The amplitude of enamel folding is high and the spacing between the folds tight. The upper molars, in particular, are fragmented and more worn than the lower.

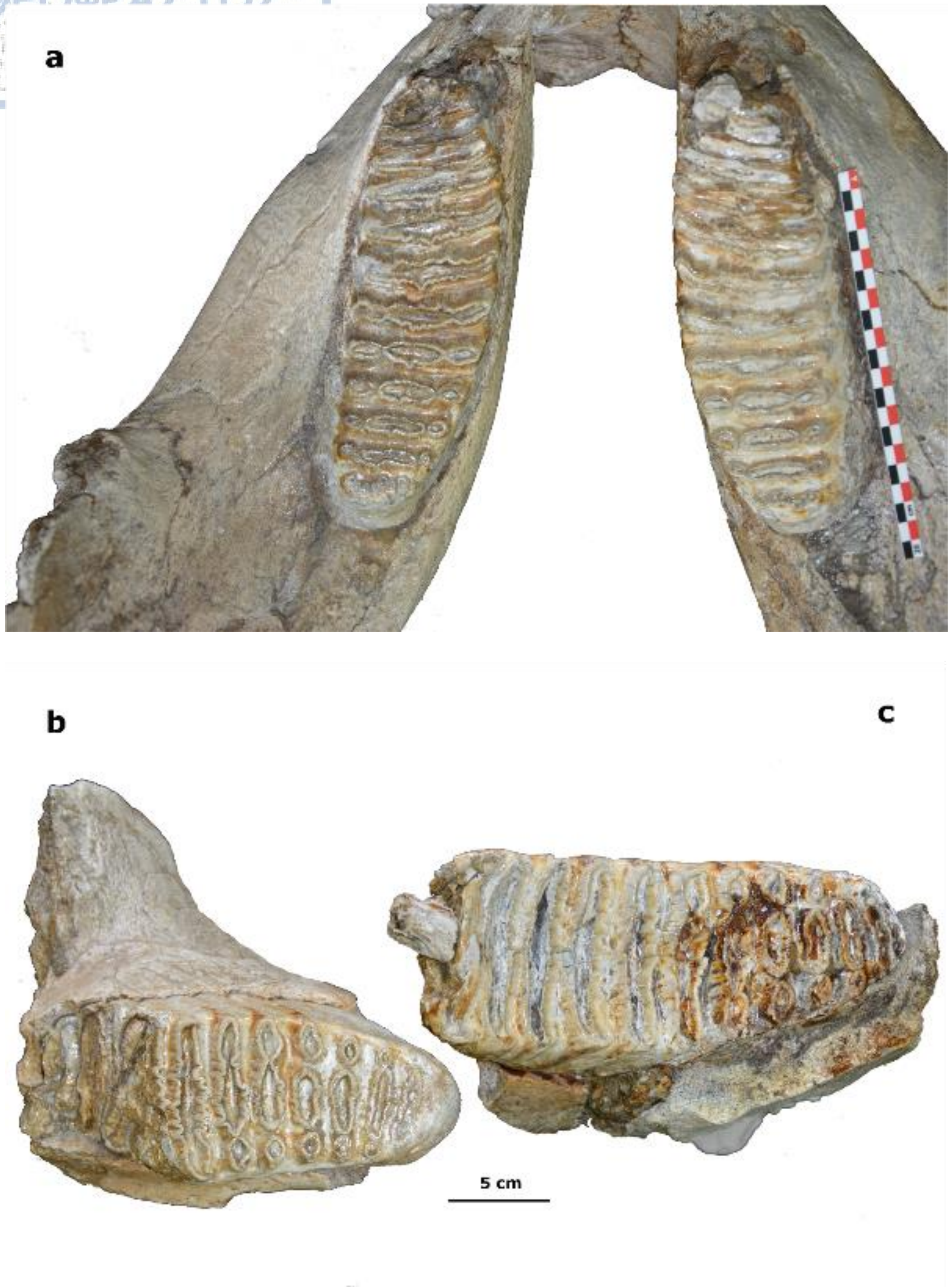

Figure 23. a) Dorsal view of the mandible bearing the left and right m2 (LGPUT-MP-02) of *Palaeoloxodon antiquus* from Tsotylion, b) ventral view of the left maxillary fragment bearing the M2, c) ventral view of the right maxillary fragment bearing the M2.

Remarks: Morphological traits of the MP-02 molars such as the presence of pointed midline sinuses, the narrow shape of the occlusal surface and the dot-dash-dot pattern in the slightly worn lamellae combined with the metric traits (ET, LF and W values) (App. Table 2) within the known range of *P. antiquus* for the m2 and M2 allow for an attribution to this species. This is also supported by the absence of medial mental foramen (Ferretti and Debruyne, 2011).

Locality: Philippi, Drama basin, Eastern Macedonia.

Age: Precise locality and stratigraphic horizon unknown Early Pleistocene.

Material examined: Right m3, LGPUT-MP-27.

Description: MP-27 is fragmented, with the distal end missing. It consists of six plates, all in use and worn. Its shape is parallel-sided with the greatest width observed at the crown. There is weak plate inclination. The lamellae are open; the shape of the enamel figures is parallel-sided with the median area folded and the lateral sides intermediate. The lateral sides of the enamel figures turn mesially. The medial edges are separated. Enamel folding is regular and strong with low amplitude and tight spacing between the folds, which extend throughout the loop.

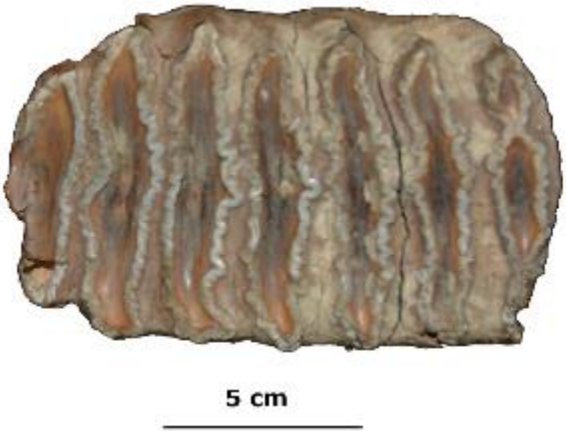

Figure 24. Occlusal view of the right m2 (LGPUT-MP-27) of *Palaeoloxodon antiquus* from Philippi.

Remarks: MP-27 was first described and attributed to *Mammuthus trogontherii* by Koulidou (2013). Judging from morphological (presence of pointed midline sinuses, intensively folded enamel of the lamellae) and metrical (narrow crown; the width stands below the lower limit for the m2 of *M. trogontherii* from Süßenborn) traits, the molar probably belongs instead to *P. antiquus*.

Locality: Pentavrysos

Age: Precise locality and stratigraphic horizon unknown (Middle–Late Pleistocene based on the presence of *P. antiquus*).

Material examined: PHP/-, left maxillary fragment with M3.

Description: The molar has an elliptic shape with the widest part being in the middle, while there is no curvature (Fig. 25). The greatest height is observed at the distal end, while the greatest tooth width is at ½ from the tooth base. The lateral edges of the plate are high and slightly bowed out. There are a few apical digitations (2) and the first complete enamel loop appears slowly. There is a single column at the distal end of the molar. Enamel height above the cement is low. The enamel figures are parallel-sided with a median loop present at two of them and their lateral sides are rounded. The enamel is even, with no direction to either the mesial or distal end. The medial edges are separated, and the enamel folding is irregular with the folds placed throughout the entire length of the enamel figure.

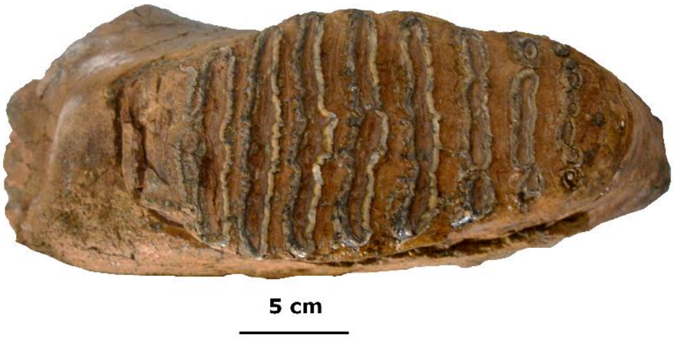

Figure 25. Ventral view of the left maxillary fragment bearing the M3 of *Palaeoloxodon antiquus* from Pentavrysos.

Remarks: The metrical values of the Pentavrysos molar are within the range of both *P. antiquus* and *M. trogontherii.* The classification to *P. antiquus* is justified by the presence of midline sinuses and the "dot-dash-dot" pattern at the distal end of the molar which is at an early stage of wear.

Locality: Wider region of Siatista, Western Macedonia.

Age: Precise locality and stratigraphic horizon unknown (Middle–Late Pleistocene based on the presence of *P. antiquus*).

Material examined: (all HPCS) M2**:** SIA-1, SIA-2, SIA-12 (right and left); M3: SIA 5, SIA 8, SIA-10; m3: SIA-21.

Remarks: The specimens of the Siatista collection were presented by Mol et al. (2010). All examined molars belong to *P. antiquus* and share the morphological and metrical characteristics of this species: pointed midline sinuses, high hypsodonty values, narrow lamellae, and width and ET values within the range of *P. antiquus* given by Maglio (1973).

Locality: Amyntaio, Ptolemais Basin, Western Macedonia.

Age: early Middle Pleistocene.

Material examined: Maxilla with right and left M3, PHP-AME-011, and associated mandible with right and left m3, PHP-AME-012.

Remarks: The maxilla and the mandible belong to the partial elephant skeleton of *P. antiquus* described in detail in Kevrekidis and Mol (2015).

Locality: Kyparissia 3, Megalopolis Basin, Peloponnese.

Age: early Middle Pleistocene.

Material examined: Right mandible fragment with m3, EPS-KYP3-160; left M3, EPS-KYP3-1289.

Remarks: The mandible KYP3-160 was described in detail in Athanassiou (2018) and based on morphological and metrical traits it was attributed to *P. antiquus*. KYP3-1289 is a still unpublished M3 that also shows the typical traits of this species.

Locality: Marathousa 1, Megalopolis Basin, Peloponnese.

Age: 500–400 ka, MIS 12, Middle Pleistocene.

Material examined: Cranium with left and right M3; AMPG-MAR-1A-942/676-6 (the elephant skeleton is collectively recorded as MAR-1A-5).

Remarks: The examined molars belong to the complete cranium of the partial elephant skeleton (Konidaris et al., 2018). The relatively narrow crown, the intensively folded enamel of the lamellae and the presence of pointed midline sinuses on the molars permit the allocation to *P. antiquus* (Konidaris et al., 2018). Further details can be found in the latter article.

Locality: several sites in the Megalopolis Basin, Peloponnese.

Age: late Middle (–Late?) Pleistocene.

Material examined: (all AMPG) left and right M3, MEG 1960/70; left M2, MEG 1960/69; left M2, MEG 1960/71; left M1, MEG 1960/80; left M3, MEG 1960/75; left M3, MEG 1960/72; left M3, MEG 1960/82; right m3, MEG 1960/77; mandible with left and right m1, 1964/44; MEG 1960/27 dex and MEG 1960/27 sin; cranium with left and right M3, AMPG-1964/445 dex AMPG-1964/445 sin.

Remarks: The Megalopolis proboscidean specimens that comprise the old collection were studied by Melentis (1961, 1965) and were attributed to various proboscidean taxa: *Palaeoloxodon antiquus antiquus*, *P. antiquus italicus*, *P. melitensis*, *Archidiskodon meridionalis meridionalis*, *A. meridionalis cromerensis*, and *Mammonteus primigenius primigenius*. However, subsequent research reclassified most of them as *Palaeoloxodon antiquus* (Lyras, 2007; Iliopoulos et al., 2010; Athanassiou, 2022).

Locality: Roupaki, Penios River basin.

Age: Late Pleistocene.

Material examined: Right M3, AMPG-ΠΝ- 4**;** left M3, AMPG-ΠΝ-5.

Remarks: The two molars (as well as an upper tusk) belong to the same individual (Athanassiou, 2000), showing the typical traits of *P. antiquus*.

5. Dental Mesowear analysis – Results

Dental mesowear angle analysis was conducted on 61 molars (34 upper, and 27 lower molars), representing 46 individuals. The dataset includes 3 molars (3 individuals) of *M. rumanus*, 10 molars (10 individuals) of *M. meridionalis*, 11 molars (8 individuals) of *M. trogontherii*, and 37 molars (25 individuals) of *P. antiquus*. The detailed results, categorized by locality and taxon, are illustrated in Figure 26.

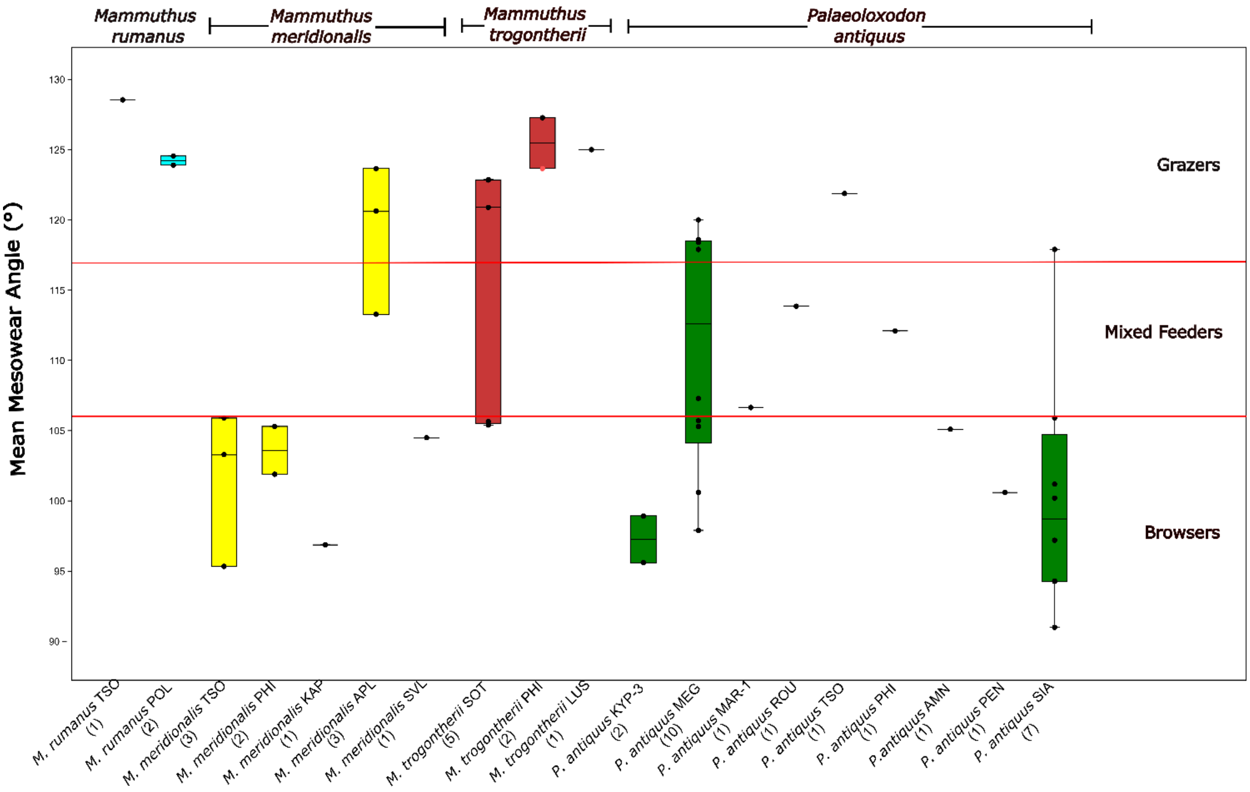

Figure 26. Box-and-whisker plots of mean mesowear angles (°) of proboscideans (*Mammuthus* spp. and *Palaeoloxodon antiquus*) from several localities of Greece. Red horizontal lines represent the boundaries between the dietary categories (106° for browsers/mixed feeders, and 117° for mixed feeders/grazers), black horizontal lines represent the median values, boxes represent the 25 and 75 percentiles (interquartile range), jitters represent each individual specimen's MMA and whiskers represent the maximum–minimum values. TSO: Tsotylion; POL: Polylakkos; PHI: Philippi; KAP: Kapetanios; APL: Apollonia-1, SOT: Sotiras; LUS: Loussika; MEG: Megalopolis (old collection); MAR-1: Marathousa 1; ROU: Roupaki; AMN: Amyntaio; KYP-3: Kyparissia 3; SVL: Symvoli; SIA: Siatista; PEN: Pentavrysos.

Both specimens of *M.* cf. *rumanus* from Polylakkos, MP-40 and MP-07, reveal grazing feeding patterns with mean mesowear angles (MMA) 123.9° and 124.6°, respectively. Similar feeding traits are noticed in the *M. rumanus* from Tsotylion (MMA = 128.5°).

Regarding *M. meridionalis*, the specimens from Tsotylion, Philippi, Kapetanios and Symvoli reveal browsing diet, from pure browsing until the boundary browsing/grazing (95.3–105.9°). On the other hand, *M. meridionalis* from Apollonia-1 shows the highest angles among *M. meridionalis* from Greece, falling between 113.3° and 123.7° and revealing a mixed-feeding diet with a significant grazing component, i.e., a diet including mainly grasses and a percentage of softer plant material.

Mammuthus trogontherii provides as a whole higher MMA than *M. meridionalis* and covers the whole mixed and most of the grazing spectrum (the average MMA from all localities is 119.2°). In particular, the Loussika mammoth provides a MMA of 125.0°, showing a clear preference towards grazing. On the same pattern, both specimens from Philippi, and MP-45, MP-46 and MP-44 from Sotiras are classified as grazers. On the contrary, MP-42 and MP-05 from Sotiras with MMA of 105.7° and 105.4° show marginally browsing to bowzing/mixed traits. As such the Sotiras collection can be separated into two different clusters, one within the grazing range (LGPUT-MP-44, MP-45 and MP-46) and one within the browsing/mixed feeding one (LGPUT-MP-42 and MP-05).

The MMA for *Palaeoloxodon antiquus* vary from 91° (SIA-12 from Siatista) to 121.9° (MP-02 from Tsotylion), i.e., from pure browsing to grazing, with a MMA of 106.9° (mixed-feeding) across all localities. Therefore, *P. antiquus* from Greece reveals a wide range of dietary categories, depending on the locality, and additionally shows marked intra- and inter-population variation. Overall, the Siatista molars exhibit the lowest MMA, primarily consisting of individuals classified as browsers, except of SIA-2 that falls on the boundary between mixed feeders and grazers. Likewise, both KYP-3 specimens (98.9° and 95.6°), and the Pentavrysos molar (100.6°), are also classified as browsers. The elephant individual from Marathousa 1 (MMA of 106.7°) and Amyntaio (105.1°) fall almost at the boundary between mixed-feeders and browsers, and therefore these individuals can be classified as browse-dominated mixed-feeders. On the other hand, the molars from Phillipi (112.1°) and Roupaki (113.9°) are plotted within mixed feeders.

The specimens from the old collection of Megalopolis (AMPG) demonstrate a broad range of MMA, from 97.9° to 120.1°, and from a pure browsing diet to a grazing one. The specimens are separated into two clusters; one plotted as grass-dominated (AMPG-MEG 1960/69, 1960/77, 1960/75, 1960/72, and 1960/71) and one as browsing (AMPG-1964/445, and AMPG-MEG 1960/27, 1960/70, 1960/27, 1960/80, and 1960/82).

In the specimens collected from Megalopolis and Sotiras, a clear distinction in mesowear angles is observed, leading to the identification of two distinct dietary groups in each locality (one browsing and one grazing). Considering the uncertain stratigraphic origin of the specimens from both sites the presence of multiple populations, exhibiting different dietary preferences and temporal ranges within each locality, is possible.

Species	Locality	*n*	Mean mesowear angle (˚)	Mean mesowear angle range (˚)	Dietary category
Mammuthus rumanus	Tsotylion	1	126.5	–	**Gr**
Mammuthus rumanus	Pollylakos	2	126.2	123.9 – 128.5	**Gr**
Mammuthus meridionalis	Tsotylion	3	101.5	95.3 – 106.4	**Br**, Mf
Mammuthus meridionalis	Phillipi	2	105.6	105.3 – 106.0	**Br**
Mammuthus meridionalis	Kapetanios	1	96.9	–	**Br**
Mammuthus meridionalis	Apollonia-1	3	119.2	113.3 – 123.7	Mf, **Gr**
Mammuthus meridionalis	Symvoli	1	105.9	–	**Br**
Mammuthus trogontherii	Sotiras	5	115.5	105.1 – 122.9	Br, **Mf**, Gr
Mammuthus trogontherii	Phillipi	2	125.5	123.7 – 127.3	**Gr**
Mammuthus trogontherii	Loussika	1	125.0	–	**Gr**
Palaeoloxodon antiquus	Phillipi	1	112.1	–	**Mf**
Palaeoloxodon antiquus	Amyntaio	1	105.0	–	**Br**
Palaeoloxodon antiquus	Siatista	7	99.8	91.0 – 117.9	**Br**, Mf, Gr
Palaeoloxodon antiquus	Megalopolis (old collection)	10	111.4	97.9 – 120.0	Br, **Mf**, Gr
Palaeoloxodon antiquus	Marathousa 1	1	106.7	–	**Mf**
Palaeoloxodon antiquus	Roupaki	1	113.9	–	**Mf**
Palaeoloxodon antiquus	Kyparissia 3	2	97.2	95.6 – 98.9	**Br**
Palaeoloxodon antiquus	Tsotylion	1	121.9	–	**Gr**
Palaeoloxodon antiquus	Pentavrysos	1	100.6	–	**Br**

Table 1. Sample means and ranges of individual mean mesowear angles in the proboscidean assemblages from Greek Pliocene–Pleistocene localities. Bolded are the dietary categories inferred from the mean mesowear angle.

Considering all the examined samples and localities, the results show a grazing diet for *M. rumanus* and *M.* cf. *rumanus* (although the sample is limited), browsing to mixed for *M. meridionalis* but mixed to grazing for the late representative from Apollonia-1, mixed feeding to grazing for *M. trogontherii*, and a wide range for *P. antiquus* covering all dietary spectrum.

It is worth noting that in specimens comprised of molars of both left and right sides (i.e., of the same individual) there is no significant difference in the mesowear angles. Specifically, MP-05 from Tsotylion, the Loussika molars, MEG 1960/70 from Megalopolis and the upper molars from Amyntaio, all have mesowear angle value range differing less than 5°, depicting a consistent pattern of mastication and an even wear pattern between the two sides of the lower or the upper jaw. Additionally, in all the above specimens the right molar provides a greater mesowear angle. The deviation between left and right molar mean mesowear angles is slight and doesn’t lead to contradictory results, regarding dietary preferences. A slightly higher angle range is observed in the specimens MP-02 from Tsotylion, SIA-12 from Siatista, AMPG-1964/445 from Megalopolis (Lefktro), and the MAR-1 elephant. The angle disparity in these specimens ranges from 5.3° to 12.4°, revealing a preference of these individuals to chew from the left or the right side. The highest fluctuation is observed in the upper MP-02 molars from Tsotylion where the difference is ca. 16°, with the right side being more worn.

Regarding differences between the preferred mastication side, two individuals with all four molars were available (upper left and right, and lower left and right), MP-02 and the Amyntaio skull. In MP-02, the molars of the left side have a MMA of 114.7°, whereas the right-side ones have 129.1°. On the Amyntaio skull the molars of the left side have a MMA of 100.7°, whereas the right-side ones 109.0°. In both these specimens the right-side molars are more worn and present a higher MMA, indicating a preference of the individuals to chew from the right side.

In order to statistically examine whether significant differences between the dietary preferences of individuals among the localities exist, two types of analyses were performed depending on the number of available samples. In the first analysis, Mann-Whittney test was conducted with the MMA from five localities where more than three specimens of the same taxon were available (*P. antiquus* from Siatista and the Megalopolis-old collection, *M.*

meridionalis from Tsotylion and Apollonia-1, and *M. trogontherii* from Sotiras). According to this test, the SIA population differs significantly with all others, apart from the *M. meridionalis* population from Tsotylion, which shares similarities with all the comparative sample.

	M. meridionalis TSO	*M. meridionalis* APL	*M. trogontherii* SOT	*P. antiquus* MEG	*P. antiquus* SIA
M. meridionalis TSO		0.08086	0.136	0.1508	0.5394
M. meridionalis APL	0.08086		0.7656	0.1083	0.03209
M. trogontherii SOT	0.136	0.7656		0.1984	0.02327
P. antiquus MEG	0.1508	0.1083	0.1984		0.01638
P. antiquus SIA	0.5394	0.03209	0.02327	0.01638	

Table 2. Mann-Whitney test conducted for localities with more than three specimens. Highlighted are the samples with *p* values < 0.05, i.e., significantly different to each other.

In localities with only one or two specimens available for mesowear angle measurement, the z-scores were calculated. Among the significant differences that analysis showed are: a) between *M. rumanus* (Tsotylion) and *M.* cf. *rumanus* (Polylakkos) and *M. meridionalis* from Tsotylion, b) between the Kapetanios and Philippi *M. meridionalis* from that from Apollonia-1, c) between *M. trogontherii* (Loussika and Philippi) from *P. antiquus* from Siatista, and d) between *P. antiquus* from Tsotylion and Siatista. On the other hand, the analysis did not show significant difference between the *P. antiquus* specimens from Kyparissia 3 and Marathousa 1 and those from the old Megalopolis collection.

	P.antiquus SIA	*P.antiquus* MEG	*M.meridionalis* TSO	*M.meridionalis* APL-1	*M. trogontherii* SOT
M. rumanus , Tsotylion (MP-04)	3.21381733	2.061882353	4.715087719	1.755347092	1.422052402
M. cf. *rumanus* , Polylakkos (MP-07)	2.846604215	1.591764706	4.014035088	1.005628518	0.98580786
M. cf. *rumanus* , Polylakkos (MP-40)	2.770491803	1.515294118	3.9	0.883677298	0.914847162
M. meridionalis , Kapetanios (KAP-1)	-0.394262295	-1.664352941	-0.842982456	-4.187054409	-2.081509033
M. meridionalis , Philippi (MP-18)	0.574941452	-0.589411765	0.761403509	-2.472795497	-1.038209607
M. meridionalis , Philippi (MP-30)	0.488290398	-0.676470588	0.631578947	-2.61163227	-1.118995633
M. trogontherii , Loussika (LUS)	2.614637002	1.358705882	3.665087719	0.633958724	0.649202976
M. trogontherii , Philippi (MP-21)	2.641725215	1.487098039	3.857953216	0.838711695	0.888682678
M. trogontherii , Philippi (MP-22)	3.06518345	1.91254902	4.492397661	1.517198249	1.283478894
P. antiquus , Philippi (MP-27)	1.292681499	0.131705882	1.836754386	-1.322795497	-0.369050218
P. antiquus , Pentavrysos	0.046604215	-1.221411765	-0.181052632	-3.480675422	-1.624672489
P. antiquus , Tsotylion (MP-02)	2.533372365	1.277058824	3.543333333	-2.65272045	0.575451647
P. antiquus , Amyntaio (AME-011)	0.563348946	-0.702235294	0.591754386	-2.65272045	-1.212433581
P. antiquus , Kyparissia 3 (KYP3-160)	-0.254605777	-1.422862745	-0.481461988	-3.801938712	-1.811608443
P. antiquus , Kyparissia 3 (KYP3-1289)	-0.643598751	-1.813686275	-1.064269006	-4.425203252	-2.174272198
P. antiquus , Marathousa 1 (MAR-1)	0.751053864	-0.513647059	0.872982456	-2.351969981	-1.042082891

Table 3. Calculated z-scores for the mean mesowear angles (°) of proboscideans from Greek localities. When z >|1.96|, the null hypothesis that the studied specimen fits within the variation of the comparative sample is confirmed. On different case, the hypothesis can be rejected as *p* < 0.05 (in such cases the z-score cell is highlighted).

6. Comparisons and discussion

The dental mesowear angle analysis showed great variation in the feeding habits of the examined Pliocene–Pleistocene proboscideans from Greece, which overall cover the entire spectrum of dietary categories, ranging from pure browsing to pure grazing individuals. MMA range from 91° in SIA-12 of *P. antiquus* to 125° in the *M. trogontherii* individual from Loussika.

Due to the scarcity of *M. rumanus* molars in Europe, comparative data regarding its feeding habits are limited to one locality, Red Crag (UK). Moreover, in order to expand the database, the two *M.* cf. *rumanus* specimens from Polylakkos are here treated as *M. rumanus* in the mean mesowear angle results and comparisons. Based on dental microwear, the specimens from Red Crag revealed both fruit and leaf browsing behavior (Rivals et al., 2019), in accordance with the low hypsodonty that characterizes *M. rumanus* and the wet and warm climate during the Pliocene in Europe. In contrast, the Greek *M. rumanus* molars from Tsotylion and Polylakkos, show a grazing diet (however, it should be noted that LGPUT-MP-04 is heavily worn and the measurement has to be considered with caution).

It is worth noting that Tsotylion and Polylakkos are situated near Milia (Grevena Basin), a locality that documents the mammutid *Mammut borsoni* and the gomphothere *Anancus arvernesis* and is dated to the early Villafranchian, Late Pliocene (Tsoukala, 2000; Tsoukala and Mol, 2016). The presence of *M.* (cf.) *rumanus* at Tsotylion and Polylakkos might indicate a comparable age. The isotopic analysis on the *M. borsoni* from Milia revealed a browsing diet (Dotsika et al., 2014). A browsing diet is also revealed for both *M. borsoni* and *A. arvernesis* based on dental mesowear and microwear from several European localities (Saarinen and Lister, 2016; Rivals et al., 2019). A hypothesis that can be derived is that in the potential coexistence of *M. rumanus* with *M. borsoni* and *A. arvernesis* in the wider area of Tsotylion and Milia, the latter two species could have occupied the ecological niche of soft plant material, leaving the grassier areas (i.e., those with more abrasive plant material) as the only available ecospace for *M. rumanus*. This potential trophic partitioning could possibly explain the high values of MMA of *M. rumanus* in Tsotylion and Polylakkos. Nevertheless, it is noted again that the sample size is limited and the stage of wear, particularly of MP-04 is advanced.

An alternative or complementary scenario that could explain the browsing adaptations of the Red Crag *M. rumanus* might be related to age differences. In particular, the slightly more derived morphological and metrical traits of the Red Crag mammoth than the *M. rumanus* specimens from Tsotylion, Montopoli, Bosilikovski and Cernătești (Kostopoulos and Koulidou, 2015), might point to a slightly younger age. Despite that most of the *M. rumanus*-bearing localities are not securely dated, Red Crag is dated to 2.6–2.4 Ma (Lister and van Essen, 2003; Rivals et al., 2015) and therefore the Red Crag mammoth could represent one of the last *M. rumanus* populations. Therefore, late populations of primitive mammoths, like the Red Crag one, might represent a shift to a more browsing diet that took place within the north-western dispersal of *M. rumanus*. On the other hand, the Greek specimens might have retained the more mixed-feeding/grazing signal of the African primitive mammoths. Isotopic and dental mesowear analyses on *Mammuthus subplanifrons* from several sites dated in the interval ca. 6.0–3.5 Ma reveal a mixed feeding/grazing diet (de Ruiter et al., 2010; Groenewald et al., 2020; Saarinen and Lister, 2023). Therefore, the Greek specimens could represent primitive populations that have retained the more grazing signal, whereas the later Red Crag one might have modified its diet during the north-western dispersal of primitive mammoths. Alternatively, local environmental factors, and accordingly dietary adaptations related to the dietary plasticity of proboscideans might be the reason for the different signal obtained for the Greek and Red Crag specimens. More dietary research on primitive proboscideans both from Greece and the rest of Europe is certainly needed to provide safer inferences on *M. rumanus* feeding habits.

The populations of *M. meridionalis* in Europe covered the entire dietary spectrum, from localities featuring mainly pure browsers to some others consisting solely of grazers, which is confirmed both by dental microwear and mesowear analyses (Saarinen and Lister, 2016; Rivals et al., 2019). This ecological flexibility is attributed to the large sheer size of this species, a trait that granted it access both to grass and to soft leaves from the top of the trees (Saarinen and Lister, 2016), and to the prolonged time period during which *M. meridionalis* was the sole proboscidean in Europe (Lister, 2004), and has survived under diverse climatic conditions in both regional and European scale. It is worth noting, that the observed dietary variation is only present in local or regional scale, since the localities documenting *M. meridionalis* have very low intra-population variation (Rivals et al., 2019).

Similar results arise for *M. meridionalis* from the Greek localities with the localities Tsotylion, Kapetanios, Phillipi and Symvoli consisting of individuals at the browsing end of the spectrum. On the other hand, the APL specimens fall into the graze-dominated category with LGPUT-APL-686 and 687 having grazing mesowear angles and LGPUT-APL-716 mixed-feeding ones.

Apollonia-1 exhibits several distinctive faunal traits, such as the predominance of caprines and early bisons in the bovid assemblage, and the remarkable increase in the relative body size of herbivores, e.g., the large-sized species of *Equus*, the giant cervid *Praemegaceros*, and the large-sized ovibovines and bovines (Kostopoulos, 1997; Koufos and Kostopoulos, 2016; Gkeme et al., 2021). The presence of the semi-aquatic *Hippopotamus* (present at the roughly coeval and of the same stratigraphic position locality of Ravin of Voulgarakis) coupled with taxa adapted to drier/colder environments such as the bovids *Pontoceros* and *Praeovibos*, indicate moderate habitats for APL (Kahlke et al., 2011). The APL faunal assemblage is dominated by mixed feeders and grazers, the browsers have notably reduced and forest-dwelling taxa are rare, overall indicating a mainly open grassy environment (Koufos and Kostopoulos, 2016; Spassov, 2016). Such habitats of tree/open savannahs were also prevailing in the wider Balkan region (Kahlke et al., 2011).

The more open environment of APL is in agreement with the presence of *M. m. vestinus* (Konidaris et al., 2020), a subspecies that is proposed to have inhabited savannah parkland with tall trees, shrubs and grasses (Ferretti and Croitor, 2001), and its dimensions, larger than the typical morph (*M. m. meridionalis*) fit with the general size increase of herbivores at APL. Therefore, the higher MMA obtained for the APL mammoth compared to the other *M. meridionalis* from Greece, which reflect a higher grazing component in its diet, are in accordance with both the environments that is hypothesized that this subspecies inhabited, as well as with the reconstruction of the APL landscape.

In the majority of European localities *M. trogontherii* presents mixed-feeding patterns with a noteworthy preference for grazing on C_4 grasses (Saarinen and Lister, 2023). More specifically, mesowear data reveal that hard grasses consisted more than 50% of its diet, while in some specimens such as the Alaskan *M. trogontherii* this percentage reached up to 90 %, without however being considered typical for the species (Saarinen et al., 2015). It is worth noting that populations found in the North Sea and in England possess similar mixed-feeding characteristics, whereas the single sample from West Runton (England) has a mesowear angle of 143˚ that ranks it among pure grazers. Similarly, dental microwear analysis reveal mixed-feeding traits in the majority of the 13 examined localities by Rivals et al. (2019), with only the specimens from Pakefield (UK) and Trimingham (UK) bearing patterns typical for grazers. The latter authors also note that the absence of puncture pits reveals a lack of fruits in the diet. The majority of *M. trogontherii* from Greece (Loussika, Philippi and Sotiras) present grazing behavior, matching both the species' cranio-dental adaptations (shortening of the skull, increased hypsodonty of the molars) to more open habitats and its general trend to such feeding traits (Saarinen and Lister, 2016). The only exceptions are two specimens from Sotiras (LGPUT-MP-05 and MP-42) that plot at the boundary mixed feeding/browsing. None of the Greek *M. trogontherii* shows a pure browsing diet.

Palaeoloxodon antiquus exhibits on average browse-dominated mixed-feeding behavior, similar to today's African savannah elephants (Saarinen and Lister, 2016). However, in relatively open, savannah-like palaeoenvironments, such as the Ilford region in Great Britain during the MIS 7, it demonstrates a mixed feeding-pattern with a greater emphasis on grass consumption (Saarinen and Lister, 2016). In the Happisburgh Formation, molars of *P. antiquus* were discovered alongside slate slabs containing plant fossils of *Pinus sylvestris* (Scots pine), *Picea excelsa* (Norway spruce), *Betula alba* (Silver birch), and *Alnus glutinosa* (Black alder). This flora suggests a preference for browsing among these animals, different from the Pleistocene populations of Waverley Wood, where mesowear angle analysis indicates a mixed-feeding behavior in more open and moist grasslands (Saarinen et al., 2016). Such fluctuations are also confirmed by dental microwear analysis, even though most of this method's results reveal a general tendency towards grazing (Rivals et al., 2019). *Palaeoloxodon antiquus* shows a significant dietary diversity in the various investigated localities (Rivals et al., 2012). For example, microwear analyses show browsing patterns in Taubach (Germany; MIS 5e), mixed-feeding patterns in United Kingdom localities and more grazing patterns in the Megalopolis Basin (old collection). According to Rivals et al. (2012) *P. antiquus* shifted from a mixed-feeding to a browsing strategy towards the end of the Pleistocene, while on the contrary, members of the *Mammuthus* lineage shifted from browsers (*M. meridionalis*) to grazers (*M. trogontherii* and *M. primigenus*).

This wide range of MMA and accordingly the diverse feeding habits of Plio-Pleistocene proboscideans is also observed in the Greek localities. Roughly half of the Greek specimens reveal pure browsing (22 out of 46 individuals), with the rest of the material classified as mixed-feeding (7 individuals) and grazing (17 individuals). Thus, a significant interspecific variation is observed. On the other hand, a high intraspecific variation in a specific locality is limited to three sites, Sotiras (five specimens, yet from unknown stratigraphic horizon), Siatista (specimens from several localities) and Megalopolis (old collection; specimens from several localities). More specifically, MMA in the Megalopolis specimens range between 97.9° and 120.0° (standard deviation 8.3), while in Siatista specimens span from 91.0° to 117.9° (standard deviation 10.6). Accordingly, the lowest angle from Sotiras of 105.4˚ (MP-05) plots as browser and the highest one of 122.9˚ (MP-44) as grazer; however, the small sample size does not allow safe conclusions.

A particular region to examine for the palaeoecological habits of *P. antiquus* is the Megalopolis Basin and the wider Peloponnese. As noted before, MMA analysis on the old collection specimens revealed two separate clusters, one featuring angles corresponding to pure browsers and one to pure grazers.

Rivals et al. (2012) applied dental microwear analysis on 12 specimens from the same collection and concluded that *P. antiquus* showed mixed feeding dietary traits with a notable tendency towards grazing. These microwear results agree with the grazing signal (upper cluster) obtained from the mesowear analysis (Fig. 26). On the other hand, the microwear results do not coincide with the lower cluster, the browsing one. Discrepancies in the results from the two methods can be explained by the different time frame (temporal scale) that these techniques capture (Sánchez-Hernández et al., 2016). Dental mesowear reflects a longer temporal scale of months-years providing an approximation of the overall (annual) diet and of the generalized annual ecological conditions, whereas dental microwear corresponds to a short temporal scale representing the last days or weeks of the individual's life. Discrepancies between the methods can be linked to higher seasonality of the area during the corresponding time, with microwear results acting as a snapshot of the palaeoenvironmental conditions (Saarinen and Lister, 2016; Sánchez-Hernández et al., 2016). Moreover, we should also consider that the studied assemblage is not homogenous and does not correspond to a single *Palaeoloxodon* population, which is perhaps the reason that the acquired mesowear angles indicate a relatively wide diet spectrum, from pure C_3 (browsing) to C_3/C_4 mix (mixed feeding) (Table 2). Therefore, we can hypothesize that although the Megalopolis Basin *P. antiquus* consumed a relatively soft vegetation rich in C_3 plants, it was also capable of incorporating harder plant components and adapt to the seasonal, or perhaps annual, environmental changes that may have taken place during the Middle–Late Pleistocene.

The studied molars from the Megalopolis site MAR-1 belong to the partial skeleton found in Area A, which was lying at the contact of the sedimentary units UA3/UA4 and was covered by UA3. The stratigraphic sequence of MAR-1 is dated to 480–420 ka and is correlated to the glacial MIS 12. The intra-tooth multi-isotope analysis conducted in this individual indicates that the MAR-1 elephant inhabited a C_3-dominated open woodland (Roditi et al., 2024). Additionally, the latter study reveals relatively stable environmental conditions with limited seasonal fluctuations in resource availability and supports the hypothesis that the Megalopolis Basin acted as a glacial refugium for Pleistocene fauna. The results of the present mesowear analysis, which plot the MAR-1 elephant at the boundary between pure C_3 (browsing) and a browse dominated mixed-feeding diet are in agreement with the isotopic study.

This mesowear signal of the MAR-1 elephant is compatible also with the existing palaeoenvironmental data for MAR-1 that further permit the detailed reconstruction of the landscape where the *Palaeoloxodon* individual once lived. The palaeobotanical study (including carpological, phytolith and wood remains) indicates the presence of shallow water in front of a reed swamp with trees in the immediate surroundings particularly *Alnus* (black alder) and *Salix* (willows) on a flat plain (Field et al., 2018). The landscape determined for the *Palaeoloxodon*-layer was open grassland and woodland at the lake side, under generally warm environmental conditions [e.g., presence of *Brasenia schreberi* (water-shield), *Euryale ferox* (prickly waterlily), *Salvinia natans* (floating fern), as well as Palmae (palm trees); Field et al. (2018)]. For this layer the ostracod study showed the existence of a freshwater to oligohaline vegetated pond or swamp (during the summer), with water temperatures ranging from 10° to 15°C (Bludau et al., 2021). A landscape with substantial woodland components and more open areas under a temperate climate is also suggested by the large mammal fauna, which besides elephants includes deer, large bovids, hippopotamuses, beavers, and macaques (Konidaris et al., 2018, 2022). Particularly, the presence in the MAR-1 fauna of the water-dependent *Hippopotamus, Castor* and *Lutra* indicates permanent freshwater bodies perennially (Konidaris et al., 2018). The presence of important freshwater bodies is further supported by the identification of a rich avian fauna mostly adapted to a lake environment (Michailidis et al., 2018).

The available palaeoenvironmental data for KYP-3 are based on the recovered vertebrate fauna, which includes freshwater and terrestrial turtles, swan, wild boar, hippopotamus, carnivorans (hyaenids and felids), deer (fallow and red, and the giant deer *Praemegaceros*) and elephants (Athanassiou, 2018; Athanassiou et al., 2018). The overall fauna of Kyparissia indicates a woodland environment around a large lake, with more open areas, under temperate climatic conditions (Athanassiou, 2018; Athanassiou et al., 2018). Although the limited sample, the browsing mesowear signal of the KYP-3 elephants is in agreement with the existing palaeoenvironmental data.

It is worth noting that within the samples of the Megalopolis Basin (old and new collection) an increase of the grass component in the diet is observed towards the stratigraphically higher localities. Namely, KYP-3 (below Lignite II; Karkanas et al., accepted), with the most browsing signal (and thus perhaps more closed), is stratigraphically lower than the browsing/mixed-feeder elephant from MAR-1 (below Lignite III; Karkanas et al., 2018), supported also by its isotopic analysis (Roditi et al., 2024). In turn, the mixed-feeder/grazing elephants from the Isioma region (dental micro- and mesowear), from where most of the old Megalopolis specimens are considered to originate (Melentis, 1965), is placed towards the upper part of the Megalopolis sedimentary sequence (Athanassiou, 2022) and thus stratigraphically higher than MAR-1. As such, there is an overall tendency towards more grazing dietary habits of the elephants from the examined localities and consequently of a “more open” environment.

Another intriguing case pertains to the palaeoecological comparison between Loussika and the Megalopolis Basin. Both are dated to the Middle Pleistocene (Megalopolis for its most part) and are situated in rather close geographic proximity to each other, but document different species, *M. trogontherii* in Loussika and *P. antiquus* in Megalopolis [note that *M. trogontherii* is so far not reported in the Megalopolis Basin despite the old and new extensive research in several stratigraphic horizons in the basin and the sole and abundant presence of *P. antiquus* (Athanassiou, 2022 and references therein; Konidaris, pers. com.)].

More specifically, the mesowear angle analysis for the Loussika mammoth revealed a grass-dominated diet in a perhaps more open and arid environment than that of Megalopolis Basin, in particular when compared to KYP-3 and MAR-1, but also to this part of the old Megalopolis collection that shows mixed-feeding towards browsing preferences, i.e., a more wooded environment. Such palaeoenvironmental differences are already known, with *M. trogontherii* typically inhabiting colder and “more open” environments (dominated by hard plant material) than *P. antiquus* which exhibited a more browsing behavior (Saarinen and Lister, 2016).

Data from the rest of Europe reveal a significant difference in mesowear angles and eating habits between *P. antiquus* and *M. trogontherii*, which coexisted in the same area (Ilford) during the same time period (MIS 7). The mesowear analysis for *P. antiquus* indicates a browse-dominated mixed feeding pattern, whereas for *M. trogontherii* suggests a grass-dominated mixed-feeding behavior (Saarinen and Lister, 2016). Therefore, in such cases of coexistence, the only possibility of surviving is one of them to alter its feeding habits. This is known as niche partitioning and allows several taxa to inhabit the same region by utilizing different parts of the environment. Therefore, it can be reasonably assumed that when *P. antiquus* and *M. trogontherii* occasionally coexisted, they present different feeding preferences, avoiding/reducing trophic conflicts, which may also be the case for the Loussika-Megalopolis area.

In northern Greece, the only locality that features both *P. antiquus* and *M. trogontherii* is Philippi. In this locality both *M. trogontherii* individuals reveal pure grazing diet (123.7° and 127.3°), while the only *P. antiquus* specimen is sorted as a mixed feeder (MMA 112.1°). Yet, the unknown stratigraphic position of the specimens, make any discussion about niche partitioning speculative.

Recent studies show that *P. antiquus* was flexible in terms of the environments that it inhabited and accordingly of its dietary adaptations, being able to alter the vegetation it consumed, if needed or forced to (Palombo et al., 2010; Saarinen et al. 2016; Rivals et al., 2019). The most common factor that could push proboscideans out of their preferred feeding range is the gradual shift of the environment, e.g., from wooded and humid environments (with softer plant material) of the interglacials to the open and arid ones (with grasses) during the glacial epochs of the Pleistocene. For this reason, more *P. antiquus* populations are present in the Italian, Iberian and Greek peninsulas during glacial periods. Those areas acted as refugia for the migrating animals, maintaining viable temperatures throughout the glacial epochs. One of these examples is the continuous presence of *P. antiquus* in the Megalopolis Basin throughout the sedimentary sequence that includes several glacial-interglacial cycles, further confirming the refugium status of this region (Bludau et al., 2021; Konidaris et al., 2023; Roditi et al., 2024).

7. Conclusions

Dental mesowear angle analysis comprises a valuable tool in understanding the dietary preferences and behavior of elephantids and therefore contributes to the palaeoenvironmental reconstructions and interpretations. The findings presented in this thesis contribute to the growing body of knowledge on the palaeoecology of Greek proboscideans, emphasizing the need for the application of several methods for more accurately reconstructing their dietary habits.

- Considering all samples and localities, the results show a grazing diet for *Mammuthus rumanus* (although the sample is limited), browsing for *Mammuthus meridionalis* (except from the Apollonia-1 population), grazing for *Mammuthus trogontherii* (apart from the browsing cluster of the SOT specimens) and a wide range for *Palaeoloxodon antiquus* covering all the dietary spectrum.
- *Mammuthus rumanus* from Polylakkos and Tsotylion, and *M. trogontherii* from Loussika and Phillipi show the highest MMA among Greek sample and a grass-dominated diet. On the other hand, *Palaeoloxodon antiquus* from Kyparissia 3 and Siatista show the lowest MMA and pure browsing preferences.
- The southern mammoth from Apollonia-1 reveals the highest MMA among *M. meridionalis* in Greece, which indicate a diet with a significant grass component. This is in agreement with the more open character of Apollonia-1 and the presence in the faunal assemblage of open-dwellers and mixed feeders-grazers.
- In line with previous studies for *P. antiquus* from Europe, the present results show also the wide dietary range for this species, from pure browsing to grazing, depending on the

locality. The greatest range of MMA is obtained in the Megalopolis (old) and Siatista collections, yet the sample originates from different stratigraphic levels.

- In sites where other palaeodiet proxy methods have been applied (dental microwear and isotopic analysis in Megalopolis specimens), mesowear angle analysis showed similar results or in cases of discrepancies this can be perhaps explained by the different temporal scales of each method.
- The browsing to mixed feeding signal obtained for the straight-tusked elephants from Kyparissia 3 and Marathousa 1 in the Megalopolis Basin are in agreement with the existing palaeoevnironmental reconstructions for these localities, which indicate the presence of substantial woodland components with more open areas under temperate climatic conditions.
- On a similar note, the dietary differences between the *M. trogontherii* from Loussika and *P. antiquus* from the Megalopolis Basin are in agreement with the already known different dietary preferences of these two taxa.

The application of dental mesowear angle analysis in additional specimens/localities from Greece and other European localities will enhance the comparisons and the statistical analyses and strengthen the interpretations. Together with the application of diverse palaeoecological proxies will yield further insights into proboscidean dietary preferences and behavior.

References

Asevedo, L., Winck, G.R., Mothé, D., Avilla, L.S., 2012. Ancient diet of the Pleistocene gomphothere *Notiomastodon platensis* (Mammalia, Proboscidea, Gomphotheriidae) from lowland mid-latitudes of South America: Stereomicrowear and tooth calculus analyses combined. Quaternary International, Mammoths and Their Relatives 1: Biotopes, Evolution and Human Impact V International Conference, Le Puy-en-Velay, 2010 255, 42–52.

Athanassiou, A., 2011. The late Pleistocene fauna of Peneiós valley (Lárissa, Thessaly, Greece): new collected material. In: 9th Annual Meeting of the European Association of Vertebrate Palaeontologists. Herakleion, Crete, Greece, 14.

Athanassiou, A., 2018. Pleistocene vertebrates from the Kyparíssia lignite mine, Megalopolis Basin, S. Greece: Rodentia, Carnivora, Proboscidea, Perissodactyla, Ruminantia. Quaternary International, The Gates of Europe 497, 198–221.

Athanassiou, A., 2022. The Fossil Record of Continental Elephants and Mammoths (Mammalia: Proboscidea: Elephantidae) in Greece, in: Vlachos, E. (Ed.), Fossil Vertebrates of Greece Vol. 1. Springer, Cham, pp. 345–391.

Athanassiou, A., Michailidis, D., Vlachos, E., Tourloukis, V., Thompson, N., Harvati, K., 2018. Pleistocene vertebrates from the Kyparíssia lignite mine, Megalopolis Basin, S. Greece: Testudines, Aves, Suiformes. Quaternary International 497, 178–197.

Bakker, E.S., Gill, J.L., Johnson, C.N., Vera, F.W., Sandom, C.J., Asner, G.P. and Svenning, J.C., 2016. Combining paleo-data and modern exclosure experiments to assess the impact of megafauna extinctions on woody vegetation. Proceedings of the National Academy of Sciences, 113(4), 847-855.

Bludau, I.J.E., Papadopoulou, P., Iliopoulos, G., Weiss, M., Schnabel, E., Thompson, N., Tourloukis, V., Zachow, C., Kyrikou, S., Konidaris, G.E., Karkanas, P., Panagopoulou, E., Harvati, K., Junginger, A., 2021. Lake-Level changes and their paleo-climatic implications at the MIS12 Lower Paleolithic (Middle Pleistocene) site Marathousa 1, Greece. Frontiers in Earth Science 9, 668445.

Boni, G., 2022. Paleoenvironmental reconstruction based on mollusc macrofaunal analysis: a case study from the Middle Pleistocene of Megalopolis basin (Peloponnesus, Greece). Master thesis, Aristotle University of Thessaloniki, Thessaloniki.

Capalbo, C., Mazza, P.P.A., Masini, F., Savorelli, A., 2018. Palaeoecology and taphonomy of the straight-tusked elephant late Middle Pleistocene site of Poggetti Vecchi (Southern Tuscany, Italy). Alpine and Mediterranean Quaternary 31, 43–48.

Cerling, T.E., Harris, J.M., Leakey, M.G., 1999. Browsing and grazing in elephants: the isotope record of modern and fossil proboscideans. Oecologia 120, 364–374.

Cerling, T.E., Quade, J., 2013. Stable Carbon and Oxygen Isotopes in Soil Carbonates, in: Swart, P.K., Lohmann, K.C., Mckenzie, J., Savin, S. (Eds.), Geophysical Monograph Series. American Geophysical Union, Washington, D. C., pp. 217–231.

de Ruiter, D.J., Brophy, J.K., Lewis, P.J., Kennedy, A.M., Stidham, T.A., Carlson, K.B., Hancox, P.J., 2010. Preliminary investigation of Matjhabeng, a Pliocene fossil locality in the Free State of South Africa. Palaeontologia Africana 45, 11–22.

Dotsika, Chantzi, Paraskevi, Tsoukala Evangelia, Heliadis, Efstathios, 2014. Palaeoenviromental information from isotopic fingerprints of the early Villafranchian *Mammut borsoni* from Milia (Grevena, Macedonia, Greece), in: Kostopoulos, D.S., Vlachos, E., Tsoukala, E. (Eds.), VIth International Conference on Mammoths and their Relatives. Scientific Annals, School of Geology, Aristotle University of Thessaloniki, Greece, Grevena-Siatista, 10.

Doukas, C., van Kolfschoten, T., Papayianni, K., Panagopoulou, E., Harvati, K., 2018. The small mammal fauna from the palaeolithic site Marathousa 1 (Greece). Quaternary International 497, 95–107.

Drucker DG, Vercoutere C, Chiotti L, Nespoulet R, Crépin L, Conard NJ, Münzel SC, Higham T, van Der Plicht J, Lázničková-Galetová M, Bocherens H., 2015. Tracking possible decline of woolly mammoth during the Gravettian in Dordogne (France) and the Ach Valley (Germany) using multi-isotope tracking (^{13}C, ^{14}C, ^{15}N, ^{34}S, ^{18}O). Quaternary International, 359, 304–317.

Eltgen, H., 1986. Feinstratigraphisch – Fazielle Untersuchungen an Pliozän – Sedimenten im Tertiärbecken südlich Neapolis/Kozani, Nordgriechenland. IGME Geological and Geophysical Researches, Special Issue, 107–115.

Ferretti, M.P., Croitor, R.V., 2001. Functional morphology and ecology of Villafranchian proboscideans from Central Italy, in: Cavarreta, G., Gioia, P., Mussi, M., Palombo, M.R. (Eds.), The world of elephants - 1st International Congress. Consiglio Nazionale delle Ricerche, Rome, pp. 103–108.

Field, M.H., Ntinou, M., Tsartsidou, G., Van Berge Henegouwen, D., Risberg, J., Tourloukis, V., Thompson, N., Karkanas, P., Panagopoulou, E., Harvati, K., 2018. A palaeoenvironmental reconstruction (based on palaeobotanical data and diatoms) of the Middle Pleistocene elephant (*Palaeoloxodon antiquus*) butchery site at Marathousa, Megalopolis, Greece. Quaternary International 497, 108–122.

Fisher, D.C., 2009. Paleobiology and Extinction of Proboscideans in the Great Lakes Region of North America, in: Haynes, G. (Ed.), American Megafaunal Extinctions at the End of the Pleistocene, Vertebrate Paleobiology and Paleoanthropology. Springer Netherlands, Dordrecht, 55–75.

Fortelius, M., Solounias, N., 2000. Functional characterization of ungulate molars using the abrasion-attrition wear gradient: A new method for reconstructing paleodiets. American Museum Novitates 3301, 1–36.

Gheerbrant, E., Sudre, J., Cappetta, H., 1996. A Palaeocene proboscidean from Morocco. Nature 383, 68–70.

Gkeme, A., Koufos, G., Kostopoulos, D., 2021. Reconsidering the equids from the Early Pleistocene fauna of Apollonia 1 (Mygdonia Basin, Greece). Quaternary 4, 12.

Groenewald, P.A., Sealy, J., Stynder, D., Smith, K.M., 2020. Dietary resource partitioning among three coeval proboscidean taxa (*Anancus capensis*, *Mammuthus subplanifrons*, *Loxodonta cookei*) from the South African Early Pliocene locality of Langebaanweg E Quarry. Palaeogeography, Palaeoclimatology, Palaeoecology 543, 109606.

Harvati, K., Konidaris, G., Tourloukis, V., 2018. Paleoanthropology at the Gates of Europe: Recent research in Greece in the frame of the PaGE ERC Starting Grant project. Quaternary International 497.

Haynes, G., 2012. Elephants (and extinct relatives) as earth-movers and ecosystem engineers. Geomorphology 157, 99-107.

Higgins P., (2018). Isotope ecology from biominerals, in: Croft, D.A., Su, D.F., Simpson, S.W. (Eds.), Methods in Paleoecology: Reconstructing Cenozoic Terrestrial Environments and Ecological Communities. Springer, Cham, pp. 99–120.

Hoppe, K.A., Stover, S.M., Pascoe, J.R., Amundson, R., 2004. Tooth enamel biomineralization in extant horses: implications for isotopic microsampling. Palaeogeography, Palaeoclimatology, Palaeoecology, Incremental Growth in Vertebrate Skeletal Tissues: Paleobiological and Paleoenvironmental Implications 206, 355–365.

Iliopoulos, G., Lyras, G., Roussiakis, S. and Athanassiou, A., 2010. Woolly rhinos and woolly mammoths in Southern Greece? Using REE elements to trace the provenance of old museum collections. In 8th Annual Meeting of the European Association of Vertebrate Palaeontologists, Aix-en-Provence, 2010. Abstracts (Vol. 46).

Janis C., 1988. An estimation of tooth volume and hypsodonty indices in ungulate mammals, and the correlation of these factors with dietary preferences. Memoires du Museum National d' Histoire Naturelle 53, 367–387.

Kahlke, R.-D., 2014. The origin of Eurasian Mammoth Faunas (*Mammuthus–Coelodonta* Faunal Complex). Quaternary Science Reviews 96, 32–49.

Kahlke, R.-D., García, N., Kostopoulos, D.S., Lacombat, F., Lister, A.M., Mazza, P.P.A., Spassov, N., Titov, V.V., 2011. Western Palaearctic palaeoenvironmental conditions during the Early and early

Middle Pleistocene inferred from large mammal communities, and implications for hominin dispersal in Europe. Quaternary Science Reviews 30, 1368–1395.

Kaiser, T.M., Solounias, N., 2003. Extending the tooth mesowear method to extinct and extant equids. Geodiversitas 25, 321–345.

Karkanas, P., Tourloukis, V., Thompson, N., Giusti, D., Panagopoulou, E., Harvati, K., 2018. Sedimentology and micromorphology of the Lower Palaeolithic lakeshore site Marathousa 1, Megalopolis basin, Greece. Quaternary International 497, 123–136.

Karkanas, P., Tourloukis, V., Thompson, N., Giusti, D., Tsartsidou, G., Athanassiou, A., Konidaris, G., Roditi, E., Panagopoulou, E., Harvati, K., accepted. The Megalopolis Paleoenvironmental Project (MegaPal). Tübingen University Press, Tübingen.

Kevrekidis, C., Mol, D., 2016. A new partial skeleton of *Elephas* (*Palaeoloxodon*) *antiquus* Falconer and Cautley, 1847 (Proboscidea, Elephantidae) from Amyntaio, Macedonia, Greece. Quaternary International 406, 35–56.

Konidaris, G.E., Athanassiou, A., Tourloukis, V., Thompson, N., Giusti, D., Panagopoulou, E., Harvati, K., 2018. The skeleton of a straight-tusked elephant (*Palaeoloxodon antiquus*) and other large mammals from the Middle Pleistocene butchering locality Marathousa 1 (Megalopolis Basin, Greece): preliminary results. Quaternary International 497, 65–84.

Konidaris, G.E., Kostopoulos, D.S., Koufos, G.D., 2020. *Mammuthus meridionalis* (Nesti, 1825) from Apollonia-1 (Mygdonia Basin, Northern Greece) and its importance within the Early Pleistocene mammoth evolution in Europe. Geodiversitas 42, 69–91.

Konidaris, G.E., Tourloukis, V., Boni, G., Athanassiou, A., Giusti, D., Thompson, N., Syrides, G., Panagopoulou, E., Karkanas, T., Harvati, K., 2023. Marathousa 2: A new Middle Pleistocene locality in the Megalopolis Basin (Greece) with evidence of hominin exploitation of megafauna (*Hippopotamus*). PaleoAnthropology 2023, 34–55.

Kostopoulos, D.S., 1997. The Plio-Pleistocene artiodactyls (Vertebrata, Mammalia) of Macedonia 1. The fossiliferous site “Apollonia-1”, Mygdonia basin of Greece. Geodiversitas 19, 845–875.

Kostopoulos, D.S., Koulidou, I., 2015. An early mammoth maxilla from north-western Greece. Quaternary International 379, 155–163.

Koufos, G.D., Kostopoulos, D.S., 2016. The Plio-Pleistocene large mammal record of Greece: Implications for early human dispersals into Europe, in: Harvati, K., Roksandic, M. (Eds.), Paleoanthropology of the Balkans and Anatolia, Vertebrate Paleobiology and Paleoanthropology. Springer Netherlands, Dordrecht, pp. 269–280.

Koufos, G.D., Pavlides, S.B., 1988. Correlation between the continental deposits of the lower Axios Valley and Ptolemais Basin 20, 9–19.

Koufos, G.D., Syrides, G.E., Kostopoulos, D.S., Koliadimou, K.K., 1995. Preliminary results about the stratigraphy and the palaeoenvironment of Mygdonia Basin, Macedonia, Greece. Geobios, First European Palaeontological Congress 28, 243–249.

Larramendi, A., 2015. Proboscideans: Shoulder height, body mass and shape. Acta Palaeontologica Polonica. 2015, 537–574.

Laws, R. M., 1966. Age criteria for the African elephant: *Loxodonta a. africana*. African Journal of Ecology 4, 1–37.

Lee-Thorp, J.A., Sealy, J.C., van der Merwe, N.J., 1989. Stable carbon isotope ratio differences between bone collagen and bone apatite, and their relationship to diet. Journal of Archaeological Science 16, 585–599.

Lister, A.M., 1996. Evolution and taxonomy of Eurasian mammoths, in: Shoshani, J., Tassy, P. (Eds.), The Proboscidea. Oxford University Press, Oxford, pp. 203–213.

Lister, A.M., 2004. Ecological interactions of elephantids in Pleistocene Eurasia: *Palaeoloxodon* and *Mammuthus*, in: Goren-Inbar, N., Speth, J.D. (Ed.), Human paleoecology in the Levantine corridor. Oxbow books, Oxford, pp. 53–60.

Lister, A.M., 2022. Mammoth evolution in the late Middle Pleistocene: The *Mammuthus trogontherii-primigenius* transition in Europe. Quaternary Science Reviews 294, 107693.

Lister, A.M., Bahn, P., 2007. Mammoths: Giants of the Ice Age (revised edition). London, UK: Frances Lincoln.

Lister, A.M., and A.V. Sher., 2015. Evolution and dispersal of mammoths across the Northern Hemisphere. Science 350, no. 6262, 805-809.

Lister, A.M., Sher, A.V., Van Essen, H., Wei, G., 2005. The pattern and process of mammoth evolution in Eurasia. Quaternary International 126–128, 49–64.

Lister, A.M., Dimitrijević, V., Marković, Z., Knežević, S., Mol, D., 2012. A skeleton of ‘steppe’ mammoth (*Mammuthus trogontherii* (Pohlig)) from Drmno, near Kostolac, Serbia. Quaternary International 276–277, 129–144.

Lucas, P.W., Omar R., Al-Fadhalah, K., Almusallam, A.S., Henry, A.G., Michael, S., Thai, L.A., Watzke, J. Strait, D.S., and Atkins, A.G., 2013. Mechanisms and causes of wear in tooth enamel: implications for hominin diets. Journal of the Royal Society Interface 10, 20120923.

MacFadden, B.J., Higgins, P., 2004. Ancient ecology of 15-million-year-old browsing mammals within C_3 plant communities from Panama. Oecologia 140, 169–182.

Maglio, V.J., 1973. Origin and Evolution of the Elephantidae. Transactions of the American Philosophical Society 63, 1.

Mainland, I.L., 2003. Dental microwear in grazing and browsing Gotland sheep (*Ovis aries*) and its implications for dietary reconstruction. Journal of Archaeological Science 30, 1513–1527.

Marinos, G., 1964. Beiträge zur Kenntnis der Verbreitung des Pleistozäns in Mazedonien. Scientific Annals, Faculty of Physics and Mathematics, University of Thessaloniki 9, 95–111.

Markov, G.N., 2012. Mammuthus rumanus, early mammoths, and migration out of Africa: some interrelated problems. Quaternary International, 276,23-26.

Melentis J.K., 1961. Die Dentition der pleistozänen Proboscidier des Beckens von Megalopolis im Peloponnes (Griechenland). Annales Oeologiques Des Pays Helleniques 12, 153–262.

Melentis J.K., 1965. Erster Fund von *Palaeoloxodon antiquus germanicus* in den jungpleistozänen Ablagerungen des Beckens von Megalopolis (Peloponnes). Praktika Akadimias Athinwn 40, 197–207. (in Greek)

Melentis J.K., 1966. *Archidiskodon meridionalis* proarchaicus n. ssp., die geologisch ältesten Elefantenreste aus Griechenland. Annales Géologiques des Pays Helléniques 17, 211–220.

Michailidis, D., Konidaris, G.E., Athanassiou, A., Panagopoulou, E., Harvati, K., 2018. The ornithological remains from Marathousa 1 (Middle Pleistocene; Megalopolis Basin, Greece). Quaternary International 497, 85–94.

Mol, D., Tsoukala, E., Batsi, A. (2010). A *Stegodon* from the area of Siatista (Kozani, Macedonia, Greece), the first evidence of the presence of Stegodon in Europe, in: 5th International conference on mammoths and their relatives Le Puy-en-Velay. Quaternaire, sp. vol. 102, 85–87.

Muttoni, G., Scardia, G., Dimitrijević, V., Kent, D.V., Monesi, E., Mrdjić, N., Korać, M., 2015. Age of *Mammuthus trogontherii* from Kostolac, Serbia, and the entry of megaherbivores into Europe during the Late Matuyama climate revolution. Quaternary Research 84, 439–447.

Muttoni, G., Scardia, G. and Kent, D.V., 2018. Early hominins in Europe: The Galerian migration hypothesis. Quaternary Science Reviews, 180, 1-29.

Owen-Smith, N., 1987. Pleistocene extinctions: the pivotal role of megaherbivores. Paleobiology 13, 351–362.

Palombo, M.R., Albayrak, E., Marano, F., 2010. The straight-tusked elephants from Neumark-Nord. A glance into a lost world, in: Meller, H. (Ed.), Elefantenreich. Eine Fossilwelt in Europa. Landesamt für Denkmalpflege und Archäologie Sachsen-Anhalt (Halle), Halle (Saale), pp. 219–247.

Panagopoulou, E., Tourloukis, V., Thompson, N., Konidaris, G., Athanassiou, A., Giusti, D., Tsartsidou, G., Karkanas, P., Harvati, K., 2018. The Lower Palaeolithic site of Marathousa 1, Megalopolis, Greece: Overview of the evidence. Quaternary International 497, 33–46.

Psarianos, P. (1958). Neue Proboscidierreste aus dem Pleistozän von Mazedonien (Griechenland). Annales geologiques des pays Helleniques 9, 221–225.

Rabinovich, R., Lister, A.M., 2017. The earliest elephants out of Africa: Taxonomy and taphonomy of proboscidean remains from Bethlehem. Quaternary International 445, 23–42.

Rivals, F., Semprebon, G.M., 2006. A comparison of the dietary habits of a large sample of the Pleistocene pronghorn *Stockoceros onusrosagris* from the Papago Springs Cave in Arizona to the modern Antilocapra americana. Journal of Vertebrate Paleontology 26, 495–500.

Rivals, F., Mihlbachler, M.C., Solounias, N., 2007. Effect of ontogenetic-age distribution in fossil and modern samples on the interpretation of ungulate paleodiets using the mesowear method. Journal of Vertebrate Paleontology 27, 763–767.

Rivals, F., Semprebon, G., Lister, A., 2012. An examination of dietary diversity patterns in Pleistocene proboscideans (*Mammuthus*, *Palaeoloxodon*, and *Mammut*) from Europe and North America as revealed by dental microwear. Quaternary International 255, 188–195.

Rivals, F., Semprebon, G.M., Lister, A.M., 2019. Feeding traits and dietary variation in Pleistocene proboscideans: A tooth microwear review. Quaternary Science Reviews 219, 145–153.

Rivals, F., Mihlbachler, M.C., Solounias, N., Mol, D., Semprebon, G.M., de Vos, J., Kalthoff, D.C., 2010. Palaeoecology of the Mammoth Steppe fauna from the late Pleistocene of the North Sea and Alaska: Separating species preferences from geographic influence in paleoecological dental wear analysis. Palaeogeography, Palaeoclimatology, Palaeoecology 286, 42–54.

Roditi, E., Bocherens, H., Konidaris, G.E., Athanassiou, A., Tourloukis, V., Karkanas, P., Panagopoulou, E., Harvati, K., 2024. Life-history of *Palaeoloxodon antiquus* reveals Middle Pleistocene glacial refugium in the Megalopolis basin, Greece. Scientific Reports 14, 1390.

Saarinen, J., Lister, A.M., 2016. Dental mesowear reflects local vegetation and niche separation in Pleistocene proboscideans from Britain. Journal of Quaternary Science 31, 799–808.

Saarinen, J., Lister, A.M., 2023. Fluctuating climate and dietary innovation drove ratcheted evolution of proboscidean dental traits. Nature Ecology and Evolution 7, 1490–1502.

Saarinen, J., Karme, A., Cerling, T., Uno, K., Säilä, L., Kasiki, S., Ngene, S., Obari, T., Mbua, E., Manthi, F.K., Fortelius, M., 2015. A new tooth wear–based dietary analysis method for Proboscidea (Mammalia). Journal of Vertebrate Paleontology 35, e918546.

Sánchez-Hernández, C., Rivals, F., Blasco, R., Rosell, J., 2016. Tale of two timescales: Combining tooth wear methods with different temporal resolutions to detect seasonality of Palaeolithic hominin occupational patterns. Journal of Archaeological Science: Reports 6, 790–797.

Saegusa H, Gilbert WH, 2008. Elephantidae. Homo erectus. Pleistocene Evidence from the Middle Awash, Ethiopia. University of California Press, Berkeley, Los Angeles, London, 193-226.

Sanders, W.J., Gheerbrant, E, Harris, J.M, Saegusa, H., Delmer, C., 2010. Cenozoic mammals of Africa, 161.

Shoshani, J., 1998. Understanding proboscidean evolution: a formidable task. Trends in Ecology & Evolution 13, 480–487.

Shoshani, J., Tassy, P., 2005. Advances in proboscidean taxonomy & classification, anatomy & physiology, and ecology & behavior. Quaternary International 126–128, 5–20.

Solounias, N., Semprebon, G., 2002. Advances in the reconstruction of ungulate ecomorphology with application to early fossil equids. novi 2002, 1–49.

Spassov, N., 2016. Southeastern Europe as a route for the earliest dispersal of *Homo* toward Europe: ecological conditions and the timing of the first human occupation of Europe, in: Harvati, K., Roksandic, M. (Eds.), Paleoanthropology of the Balkans and Anatolia, Vertebrate Paleobiology and Paleoanthropology. Springer Netherlands, Dordrecht, pp. 281–290.

Sponheimer, M., Lee-Thorp, J.A., 1999. Oxygen isotopes in enamel carbonate and their ecological significance. Journal of Archaeological Science 26, 723–728.

Steenbrink, J., Hilgen, F.J., Krijgsman, W., Wijbrans, J.R., Meulenkamp, J.E., 2006. Late Miocene to Early Pliocene depositional history of the intramontane Florina–Ptolemais–Servia Basin, NW Greece: Interplay between orbital forcing and tectonics. Palaeogeography, Palaeoclimatology, Palaeoecology, Late Miocene to Early Pliocene Environment and Climate Change in the Mediterranean Area 238, 151–178.

Steensma, K.J. (1988). Plio-/Pleistozane Großsäugetiere (Mammalia) aus dem Becken von Kastoria / Grevena, südlich von Neapolis - NW Griechenland – Inaugural Dissertation - Technische Universität Clausthal, Clausthal.

Stuart, A.J., 2005. The extinction of woolly mammoth (Mammuthus primigenius) and straight-tusked elephant (Palaeoloxodon antiquus) in Europe. Quaternary International, 126, 171-177.

Stuart, A.J., Lister, A.M., 2012. Extinction chronology of the woolly rhinoceros *Coelodonta antiquitatis* in the context of late Quaternary megafaunal extinctions in northern Eurasia. Quaternary Science Reviews 51, 1–17.

Stuart, A.J., Sulerzhitsky, L.D., Orlova, L.A., Kuzmin, Y.V., Lister, A.M., 2002. The latest woolly mammoths (*Mammuthus primigenius* Blumenbach) in Europe and Asia: a review of the current evidence. Quaternary Science Reviews 21, 1559–1569.

Teeri, J.A., Stowe, L.G., 1976. Climatic patterns and the distribution of C_4 grasses in North America. Oecologia 23, 1–12.

Todd, N.E., 2010. Qualitative comparison of the cranio-dental osteology of the extant elephants, Elephas maximus (Asian elephant) and Loxodonta africana (African elephant). The Anatomical Record: Advances in Integrative Anatomy and Evolutionary Biology 293, no. 1, 62-73.

Tourloukis, V., Muttoni, G., Karkanas, P., Monesi, E., Scardia, G., Panagopoulou, E., Harvati, K., 2018a. Magnetostratigraphic and chronostratigraphic constraints on the Marathousa 1 Lower Palaeolithic site and the Middle Pleistocene deposits of the Megalopolis basin, Greece. Quaternary International, The Gates of Europe 497, 154–169.

Tourloukis, V., Thompson, N., Panagopoulou, E., Giusti, D., Konidaris, G.E., Karkanas, P., & Harvati, K., 2018b. Lithic artifacts and bone tools from the Lower Palaeolithic site Marathousa 1, Megalopolis, Greece: Preliminary results. Quaternary International, 497, 47–64.

Tsoukala, E., Lister, A., 1998. Remains of straight-tusked elephant, *Elephas* (*Palaeoloxodon*) *antiquus* Falc. & Caut. (1847) ESR-dated to oxygen isotope Stage 6 from Grevena (W Macedonia, Greece). Bolletino-Societa Paleontologic Italiana 37, 117–140

Tsoukala, E., Mol, D., Pappa, S., Vlachos, E., van Logchem, W., Vaxevanopoulos, M., Reumer, J., 2011. *Elephas antiquus* in Greece: new finds and a reappraisal of older material (Mammalia, Proboscidea, Elephantidae). Quaternary International 245, 339–349.

Tsoukala, E., Mol, D., 2016. The Proboscidea of the Early Villafranchian site of Milia (Grevena, Macedonia, Greece). Quaternary International 406, 4–24.

Tzedakis P.C., Hooghiemstra H., Pälike H., 2006. The last 1.35 million years at Tenaghi Philippon: revised chronostratigraphy and long-term vegetation trends. Quaternary Science Reviews 25, 3416–3430.

Van Essen, J.A., 2011. Tracing transitions: an overview of the evolution and migrations of the genus *Mammuthus* Brookes, 1828 (Mammalia, Proboscidea). Universiteit Leiden.

van Vugt, N., Langereis, C.G., Hilgen, F.J., 2001. Orbital forcing in Pliocene–Pleistocene Mediterranean lacustrine deposits: dominant expression of eccentricity versus precession. Palaeogeography, Palaeoclimatology, Palaeoecology 172, 193–205.

Vinken, 1965. Stratigraphie und Tektonik des Beckens von Megalopolis (Peloponnes, Griechenland). Geologisches Jahrbuch 83, 97–148.

Wei, G., Hu, S., Yu, K., Hou, Y., Li, X., Jin, C., Wang, Y., Zhao, J. and Wang, W., 2010. New materials of the steppe mammoth, Mammuthus trogontherii, with discussion on the origin and evolutionary patterns of mammoths. Science China Earth Sciences, 53,956-963.

Appendix

Appendix Table 1. Comparison of the range and mean values for the m2 of various European proboscideans compared to specimens studied in this thesis. Data from Maglio (1973) and Lister (2022).

m2	Locality		ET	LF	PN	W	W with/added cement
M. meridionalis	Upper Valdarno	min	2.4	4.6	8	69	
		mean	2.8 (10)	5.1 (10)	9.3 (6)	85.1 (10)	
		max	3.5	6.1	10	97	
M. trogontheirii	Süßenborn	min	1.6	5.49	11	70	
		mean	1.95 (12)	6.275 (12)	12.1 (11)	82 (11)	
		max	2.5	8	14	92.5	
M. primigenus	Předmostí	min	1.3	6.81	12	72	
		mean	1.53 (29)	8.2 (29)	14.04 (44)	84.5 (30)	
		max	1.8	9.83	16	99	
P. antiquus	Several Localities	min	1.8	4.9	9	53	
		mean	2.2 (11)	5.7 (11)	11.2 (10)	65 (11)	
		max	2.5	6.9	13	80.2	
M. cf. *rumanus*	Polylakkos	MP-40	4.37	3.85	>4	87.08	87.08
M. cf. *rumanus*	Polylakkos	MP-07	3.57	3.855	>7	99.8	99.8
M. meridionalis	Tsotylion	MP-43	2.705	4.94	>10	74.39	79.39
M. meridionalis	Tsotylion	MP-17	3.17	4.67	>8	78.81	78.81
M. trogontherii	Sotiras	MP-42	2.84	6.88	12	81.4	81.4
M. trogontherii	Sotiras	MP-05 sin	3.24	7.01	13	87.04	95.82
M. trogontherii	Sotiras	MP-05 dex	3.39	6.91	14	85.68	90.68
P. antiquus	Tsotylion	MP-02 sin	2.45	4.34	11	76	76
P. antiquus	Tsotylion	MP-02 dex	2.43	4.26	12	72	72
P. antiquus	Philippi	MP-27	2.464	5.11	>5	68.13	73.13

Appendix Table 2. Comparison of range and mean values for the M2 of various European proboscideans compared to specimens studied in this thesis. Data from Maglio (1973) and Lister (2022).

M2	Locality		ET	LF	PN	W	W with/added cement
M. meridionalis	Upper Valdarno	min	2.4	4	8	76	
		mean	2.8 (17)	5.1 (18)	9.7 (14)	86.8 (18)	
		max	3.5	5.7	11	105.7	
M. trogontheirii	Süßenborn	min	1.9	5.72	11	83	
		mean	2.15(29)	7.4 (30)	12.5 (20)	91.7 (29)	
		max	2.9	8.74	14	102	
M. primigenus	Předmostí	min	1.1	7.7	12	75	
		mean	1.42 (30)	9.51 (31)	14.38 (13)	84.6 (31)	
		max	1.7	11.04	16	955	
P. antiquus	Several Localities	*min*	1.8	4.9	9	53	
		mean	2.2	5.7	11.2	65	
		max	2.5	6.9	13	80.2	
M. rumanus	Tsotylion	MP-04	3.702	-	>4	107.25	107.25
M. trogontherii	Sotiras	MP-45	2.56	6.46	9	85.79	90.79
P. antiquus	Tsotylion	MP-02 sin	2.69	6.02	>11	81	81
P. antiquus	Tsotylion	MP-02 dex	3.34	6.06	>10	79	79

Appendix Table 3. Comparison of range and mean values for the m3 of various European proboscideans compared to specimens studied in this thesis. Data from Maglio (1973), Lister et al. (2012), and Konidaris et al. (2020).

m3	Locality		ET	LF	PN	W	W with/added cement
M. meridionalis	Upper Valdarno	min	2.2	3.62	10	77	
		mean	3.08 (16)	4.75 (16)	12.8 (16)	96.8 (16)	
		max	4.3	6.11	15	119	
M. trogontheirii	Süßenborn	min	2	4.45	17	83	
		mean	2.46 (17)	5.27 (17)	19 (17)	97.7 (17)	
		max	3	6.84	21	118	
M. primigenus	Předmostí	min	1.3	6.17	19	75	
		mean	1.53 (27)	7.56 (31)	22.8 (11)	90.3 (31)	
		max	2	9.13	27	107	
P.antiquus	Several Localities	min	1.8	4.4	13	50	
		mean	2.6 (12)	5.7 (12)	15.4 (9)	72.3 (12)	
		max	3.4	6.8	18	88	
M. cf. *rumanus*	Polylakkos	MP-40	4.37	3.85	>4	87.08	87.08
M. meridionalis	Kapetanios	KAP-1	3.41	5.1	>11	118	123
M. meridionalis	Philippi	MP-30	3.513	5.14	>5	77.3	82.3
M. meridionalis	Philippi	MP-18	3.95	4.18	>4	73.54	73.54
M. meridionalis	Apollonia-1	APL-687	3.24	3.76	>8	88.8	88.8
M. meridionalis	Apollonia-1	APL-716	3.1	4.6	>12	102	102
M. trogontherii	Sotiras	MP-46	2.62	4.72	>16	85.92	85.92
M. trogontherii	Philippi	MP-21	2.08	5.57	>12	83.76	83.76
M. trogontherii	Philippi	MP-22	2.466	5.19	15	81.91	81.91
M. trogontherii	Sotiras	MP-44	3.81	4.8	>9	98.46	98.46
P. antiquus	Pentavrysos		2.9	5.92	>11	109.2	109.2

Appendix Table 4. Comparison of range and mean values for the M3 of various European proboscideans compared to specimens studied in this thesis. Data from Maglio (1973), Lister et al. (2012), and Konidaris et al. (2020).

M3	Locality		ET	LF	PN	W	W with/added cement
		min	3	3	8		
M. rumanus	Several Localities	mean	3.7	4.1	8.7	95	
		max	4.5	4.72	10		
		min	2.5	4.2	12	80	
M. meridionalis	Upper Valdarno	mean	3.1 (16)	5.3 (16)	12.8 (16)	104.9 (16)	
		max	3.8	6.4	14-15	127	
		min	1.7	5.8	17	77	
M. trogontheirii	Süßenborn	mean	2.4 (20)	7 (20)	19.7 (20)	101.6 (20)	
		max	3	8.9	22	123	
		min	1.2	7.61	20	79.5	
M. primigenus	Předmostí	mean	1.56 (40)	9.5 (44)	23 (16)	96.9 (38)	
		max	2	11.8	26	119.5	
		min	2.17	5.36	13	81.6	
P. antiquus	Several Localities	mean	2.68	6.18	16	89.2	
		max	3.19	7	19	96.8	
M. meridionalis	Tsotylion	MP-16	3.4	5.88	>8	88.72	88.72
M. meridionalis	Apollonia-1	APL-686B	2.8	5.5	>13	87	87

Appendix Table 5. Examined elephantid specimens with their mean mesowear angle, dietary category, and classification into age groups of Laws (1966).

Species	Locality	Specimen	Tooth/Teeth measured	Mean mesowear angle (°)	Dietary category	Group (Laws, 1966)
Mammuthus rumanus	Tsotylion	LGPUT-MP-04	M3 dex	128.5	Gr	XV-XVIII
Mammuthus cf. *rumanus*	Polylακkos	LGPUT-MP-07	m1/m2 sin	124.6	Gr	XIX
Mammuthus cf. *rumanus*	Polylακkos	LGPU-MP-40	m2/m3 dex	123.9	Gr	XX-XXII
Mammuthus meridionalis	Apollonia-1	LGPUT-APL 716	m3 dex	113.3	Mf	XXV-XXVI
Mammuthus meridionalis	Apollonia-1	LGPUT-APL-686B	M3 sin	123.7	Gr	XXI-XXII
Mammuthus meridionalis	Apollonia-1	LGPUT-APL 687	m3 sin	120.6	Gr	XXI-XXII
Mammuthus meridionalis	Kapetanios	LGPUT-KAP-1	m3 sin	96.9	Br	XXV-XXVI
Mammuthus meridionalis	Philippi	LGPUT-MP-18	m2 dex	105.3	Br	XXIV-XXVI
Mammuthus meridionalis	Philippi	LGPUT-MP-30	m3 dex	101.9	Br	XXIII-XXVI
Mammuthus meridionalis	Simvoli	AMPG-1964/442	M3 sin	104.5	Br	XXI-XXII
Mammuthus meridionalis	Tsotylion	LGPUT-MP-43	m2 dex	105.9	Br	XV-XVIII
Mammuthus meridionalis	Tsotylion	LGPUT-MP-17	m2 sin	103.3	Br	XV-XVIII
Mammuthus meridionalis	Tsotylion	LGPUT-MP-16	M3 sin	95.3	Br	XXII-XXVI
Mammuthus trogontherii	Loussika	Loussika	m3 dex and sin, M3 sin	125.0	Gr	XXII
Mammuthus trogontherii	Philippi	LGPUT-MP-21	m3 sin	123.7	Gr	XXIII-XXV
Mammuthus trogontherii	Philippi	LGPUT-MP-22	m3 dex	127.3	Gr	XXIII-XXV
Mammuthus trogontherii	Sotiras	LGPUT-MP-45	M2 dex	120.9	Gr	XV-XVIII
Mammuthus trogontherii	Sotiras	LGPUT-MP-42	m2 sin	105.7	Br	XVI-XVII
Mammuthus trogontherii	Sotiras	LGPUT-MP-46	m3 sin	122.8	Gr	XXIV-XXVI
Mammuthus trogontherii	Sotiras	LGPUT-MP-05	m2 dex and sin	105.4	Br	XXIV-XXVI
Mammuthus trogontherii	Sotiras	LGPUT-MP-44	m3 dex	122.9	Gr	XXVI
Palaeoloxodon antiquus	Pentavrysos	-	M3 sin	100.6	Br	XXVII
Palaeoloxodon antiquus	Kyparissia-3	EPS-KYP3-160	m3	98.9	Br	XXIII-XXIV
Palaeoloxodon antiquus	Kyparissia-3	EPS-KYP3-1289	M3	95.6	Br	XXIII-XXIV
Palaeoloxodon antiquus	Marathousa 1	AMPG-MAR 1	M3 sin and dex	106.7	Br	XXVII
Palaeoloxodon antiquus	Megalopolis (old collection)	AMPG-MEG 1960/69	M2 sin	120.0	Gr	XVIII
Palaeoloxodon antiquus	Megalopolis (old collection)	AMPG-MEG 1960/77	M3 dex	118.6	Gr	XXII
Palaeoloxodon antiquus	Megalopolis (old collection)	AMPG-MEG1960/75	M3 sin	118.5	Gr	XXVI
Palaeoloxodon antiquus	Megalopolis (old collection)	AMPG-MEG 1960/72	M3 sin	118.4	Gr	XXII
Palaeoloxodon antiquus	Megalopolis (old collection)	AMPG-MEG 1960/71	M3 sin	117.9	Gr	XXII
Palaeoloxodon antiquus	Megalopolis (old collection)	AMPG-MEG 1960/70	M3 dex and sin	105.7	Br	XXIV-XXV
Palaeoloxodon antiquus	Megalopolis (old collection)	AMPG-MEG 1960/27	M1 dex and sin	105.3	Br	X-XI
Palaeoloxodon antiquus	Megalopolis (old collection)	AMPG-MEG 1960/80	M1 sin	100.6	Br	XI-XIII
Palaeoloxodon antiquus	Megalopolis (old collection)	AMPG-MEG 1960/82	M3 sin	97.9	Br	XXIV-XXV
Palaeoloxodon antiquus	Megalopolis (old collection; Lefktro)	AMPG-1964/445	M3 dex and sin	107.3	Br	XXIII-XXV
Palaeoloxodon antiquus	Amyntaio	PHP-AME-011	M3 dex and sin, m3 dex and sin	105.1	Br	XXIV-XXV
Palaeoloxodon antiquus	Roupaki	AMPG-ΠΝ- 4, 5	M3 dex and sin	113.9	Mf	XXVII
Palaeoloxodon antiquus	Siatista	HPCS-SIA 2	M2	117.9	Gr	XV-XXI
Palaeoloxodon antiquus	Siatista	HPCS-SIA 1	M2	105.9	Br	XV-XIX
Palaeoloxodon antiquus	Siatista	HPCS-SIA 8	M3	101.2	Br	XXII-XXVII
Palaeoloxodon antiquus	Siatista	HPCS-SIA-21	m3	100.2	Br	XXII-XXVII
Palaeoloxodon antiquus	Siatista	HPCS-SIA 10	M3	97.2	Br	XXII-XXVII
Palaeoloxodon antiquus	Siatista	HPCS-SIA 5	M3	94.3	Br	XXII-XXVII
Palaeoloxodon antiquus	Siatista	HPCS-SIA 12	M2 dex and sin	91.0	Br	XV-XXI
Palaeoloxodon antiquus	Tsotylion	LGPUT-MP-02	M2 dex and sin, m2 dex and sin	121.9	Gr	XVI
Palaeoloxodon antiquus	Philippi	LGPUT-MP-27	m2 dex	112.1	Mf	XVIII-XV